

Fig. 3. Disease progression in hSOD1 (G93A) transgenic rats monitored by four effective measures. **A:** Body weight. The weight gain of the transgenic group stopped at around 110–120 days. The difference became statistically significant at 112 days of age ( $n = 9$  for each genotype). **B:** Inclined plane. The wild-type group scored 75–80° throughout the period, whereas the score of the transgenic group declined. The difference became statistically significant at 120 days of age ( $n = 9$  for each genotype). **C:** Cage activity. The movements of the wild-type group were stable, whereas the scores of the transgenic group declined. Significance was reached at 125 days of age ( $n = 8$

for each genotype). **D–F:** SCANET. For all parameters (M1, M2, RG), the movement scores of the transgenic group became constantly worse than those of the wild-type group after 60 days of age. The differences between the groups increased markedly after 90 days of age. Significance was attained beginning at 67 days of age for M1 and M2, and at 87 days of age for RG ( $n = 4$  for each genotype). The comparison between the wild-type and transgenic groups was stopped when the first of the transgenic rats reached the end-stage of the disease and was sacrificed. Mean  $\pm$  SEM. \* $P < 0.05$ . \*\* $P < 0.01$ ; two-tailed unpaired Student's  $t$ -test.

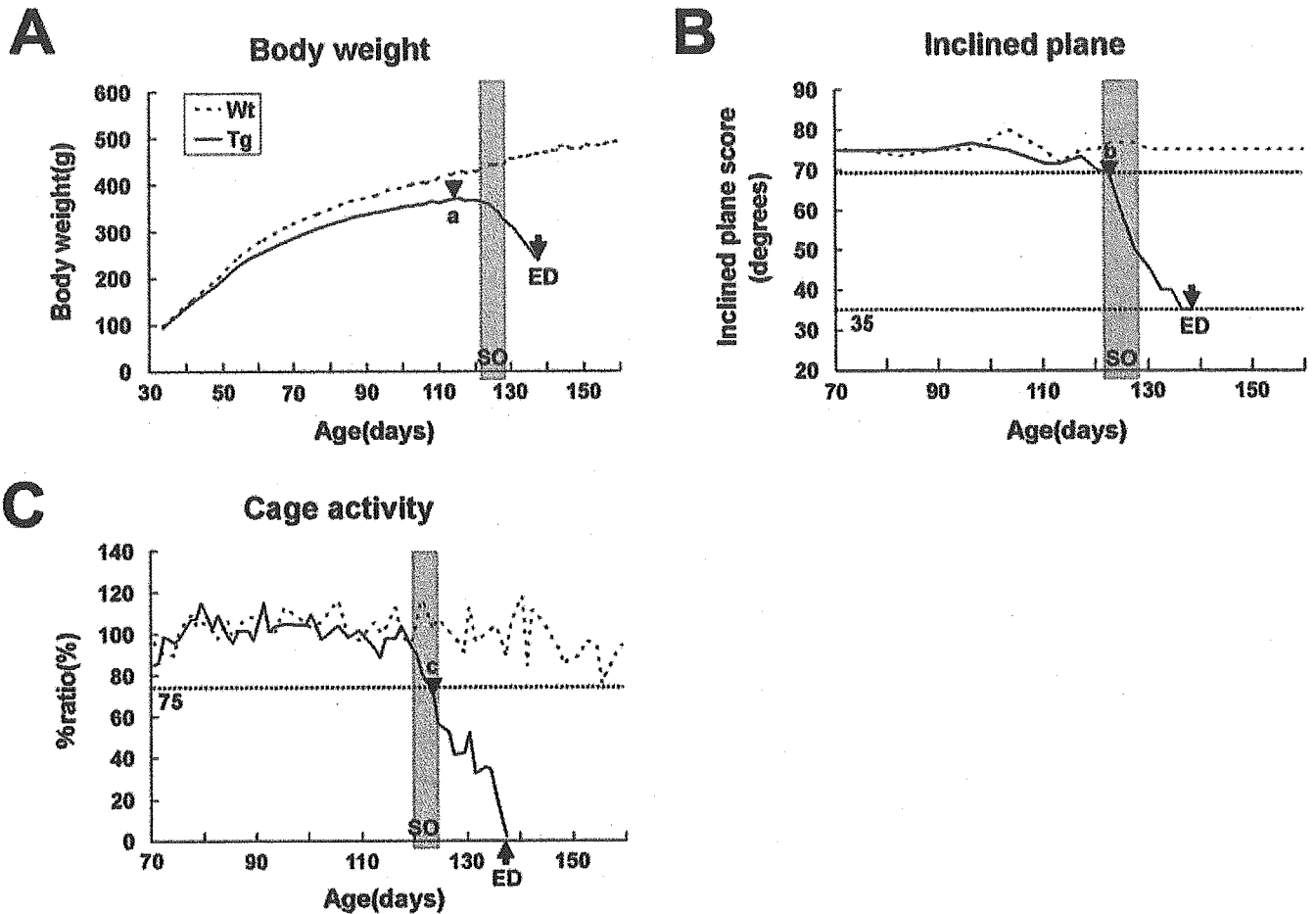


Fig. 4. Schematic presentation of the results from the body weight (A), inclined plane test (B), and cage activity (C) assessments. The onset defined by each measure (black arrowheads) and the end-stage of the disease (ED, black arrows) are indicated in the figures. a, pre-symptomatic onset: the day the transgenic rats scored their maximum body weight. b, muscle weakness onset: the earliest day the transgenic rats scored  $<70^\circ$  in the inclined plane test. c, hypo-activity

onset: the earliest day the transgenic rats scored  $<75\%$  of the mean movements from 70–90 days of age in the cage activity measure. SO, subjective onset: the earliest day that observable functional deficits such as paralysis of the limbs or symptoms of general muscle weakness were observed subjectively in the open field (the gray shaded region in A–C).

60 days of age for all parameters (M1, M2, RG), however, even after the wild-type animals showed the decrease in their movement scores. The differences between the two groups increased markedly after 90 days of age for M1, M2, and RG (Fig. 3D–F). The performance of each rat fluctuated so markedly that the SCANET test seems to be inappropriate for statistical analysis.

#### Onset, End-Stage, and Duration of Disease in hSOD1 (G93A) Transgenic Rats

Using the quantitative analysis of disease progression by body-weight measurement, the inclined plane test, and cage activity, as described above, we defined three time points of “objective onset,” as shown in Figure 4. The SCANET results did not allow us to define a time of objective onset, because we could not establish a stable baseline level using the data from the

highly variable measurements we obtained, even for wild-type rats. The righting reflex failure was useful for detecting the time point of end-stage disease, which we defined as the generalized loss of motor activity in affected rats. A total of 20 transgenic rats assessed by body weight and the inclined plane test were analyzed for the day of objective onset, end-stage, and duration of the disease. The cage activity data from the eight transgenic rats were obtained simultaneously. The results are shown in Table IV.

The day the transgenic rats reached their maximum body weight was defined as pre-symptomatic onset ( $113.6 \pm 4.8$  days of age, black arrowhead in Fig. 4A, Table IV). This onset was judged retrospectively and always preceded the subjective onset (gray shaded region, Fig. 4A), which was determined by observable functional deficits in the open field, such as paralysis of limbs and symptoms of general muscle weakness. The

**TABLE IV. Onset, End-Stage, and Duration in Days of Disease in hSOD1 (G93A) Transgenic Rats**

Evaluation methods	Body weight and inclined plane ( <i>n</i> = 20)	Cage activity ( <i>n</i> = 8)
Objective onset		
Pre-symptomatic onset <sup>a</sup>	113.6 ± 4.8 (103–124)	
Muscle weakness onset <sup>b</sup>	125.2 ± 7.4 (110–144)	
Hypo-activity onset <sup>c</sup>		122.8 ± 9.2 (109–139) <sup>c</sup>
Subjective onset (SO) <sup>d</sup>	126.5 ± 7.1 (113–147)	121.3 ± 9.8 (109–140)
End-stage disease (ED) <sup>e</sup>	137.8 ± 7.1 (128–155)	134.1 ± 8.2 (122–149)
Duration <sup>f</sup>		
ED-a <sup>g</sup>	24.3 ± 6.5	
ED-b <sup>h</sup>	12.6 ± 3.5	
ED-c <sup>i</sup>		11.4 ± 1.3

Values are means ± SD.

<sup>a</sup> Maximum of body weight.

<sup>b</sup> Less than 70 degrees in the inclined plane test.

<sup>c</sup> Less than 75% in the mean movements of 70–90 days in the cage activity.

<sup>d</sup> Observable functional deficits.

<sup>e</sup> Righting reflex failure.

<sup>f</sup> Difference in days between ED and each onset;

<sup>g</sup> between ED and pre-symptomatic onset,

<sup>h</sup> between ED and muscle weakness onset,

<sup>i</sup> between ED and hypo-activity onset.

**TABLE V. Comparison of the Onset, End-stage, and Duration in Days of Disease in the Forelimb-type and the Hindlimb-type Rats**

	Forelimb type ( <i>n</i> = 4)	Hindlimb type ( <i>n</i> = 14)	General type* ( <i>n</i> = 2)
Pre-symptomatic onset <sup>a</sup>	112.5 ± 6.7	114.6 ± 4.3	(108.5)
Muscle weakness onset <sup>b</sup>	125.8 ± 2.8	126.7 ± 7.3	(113.5)
End-stage disease (ED) <sup>c</sup>	134.0 ± 2.4	140.1 ± 7.1	(129.5)
Duration <sup>d</sup>			
ED-a <sup>e</sup>	21.5 ± 8.5	25.5 ± 6.2	(21)
ED-b <sup>f</sup>	8.3 ± 1.0	13.4 ± 3.0	(16)

Values are mean ± SD.

\* Values of general-type rats are listed in parenthesis for reference.

<sup>a</sup> Maximum of body weight.

<sup>b</sup> Less than 70 degrees in the inclined plane test.

<sup>c</sup> Righting reflex failure.

<sup>d</sup> Difference in days between ED and each onset;

<sup>e</sup> between ED and pre-symptomatic onset,

<sup>f</sup> between ED and muscle weakness onset.

pre-symptomatic onset was the most sensitive of all the onset measures described in this study (Table IV).

The first day the transgenic rats scored <70° in the inclined plane test was defined as the muscle weakness onset (black arrowhead, Fig. 4B). We could judge this onset prospectively. Muscle weakness onset (125.2 ± 7.4 days of age, Table IV) was usually recorded before or at almost the same time as the subjective onset (8 days before to 1 day after, gray shaded region, Fig. 4B and 126.5 ± 7.1 days of age, Table IV). The day the transgenic rats scored 35° or less on the inclined plane test coincided with the day of righting reflex failure (black arrow, Fig. 4B).

The first day the transgenic rats scored <75% of their baseline movements in the cage activity test was defined as hypo-activity onset (black arrowhead, Fig. 4C and 122.8 ± 9.2 days of age, Table IV). We could also judge this onset prospectively. Hypo-activity onset was

recorded 1 day before to 4 days after the subjective onset (SO, shown as the gray shaded region in Fig. 4C and 121.3 ± 9.8 days of age, Table IV). A 0% movement score for cage activity was seen at almost the same time as righting reflex failure (black arrow, Fig. 4C). Although disease onset and end-stage could be objectively defined with these methods, they had a wide range, of about 1 month, because of the diversity of the phenotypes (Table IV).

#### Differences in Disease Courses Between the Forelimb- and Hindlimb-Type Rats

Because we noticed variability in disease courses among different clinical types of hSOD1 (G93A) rats, we next assessed disease progression in 20 transgenic rats with forelimb- (*n* = 4), hindlimb- (*n* = 14), and general- (*n* = 2) type, using the probability of objective

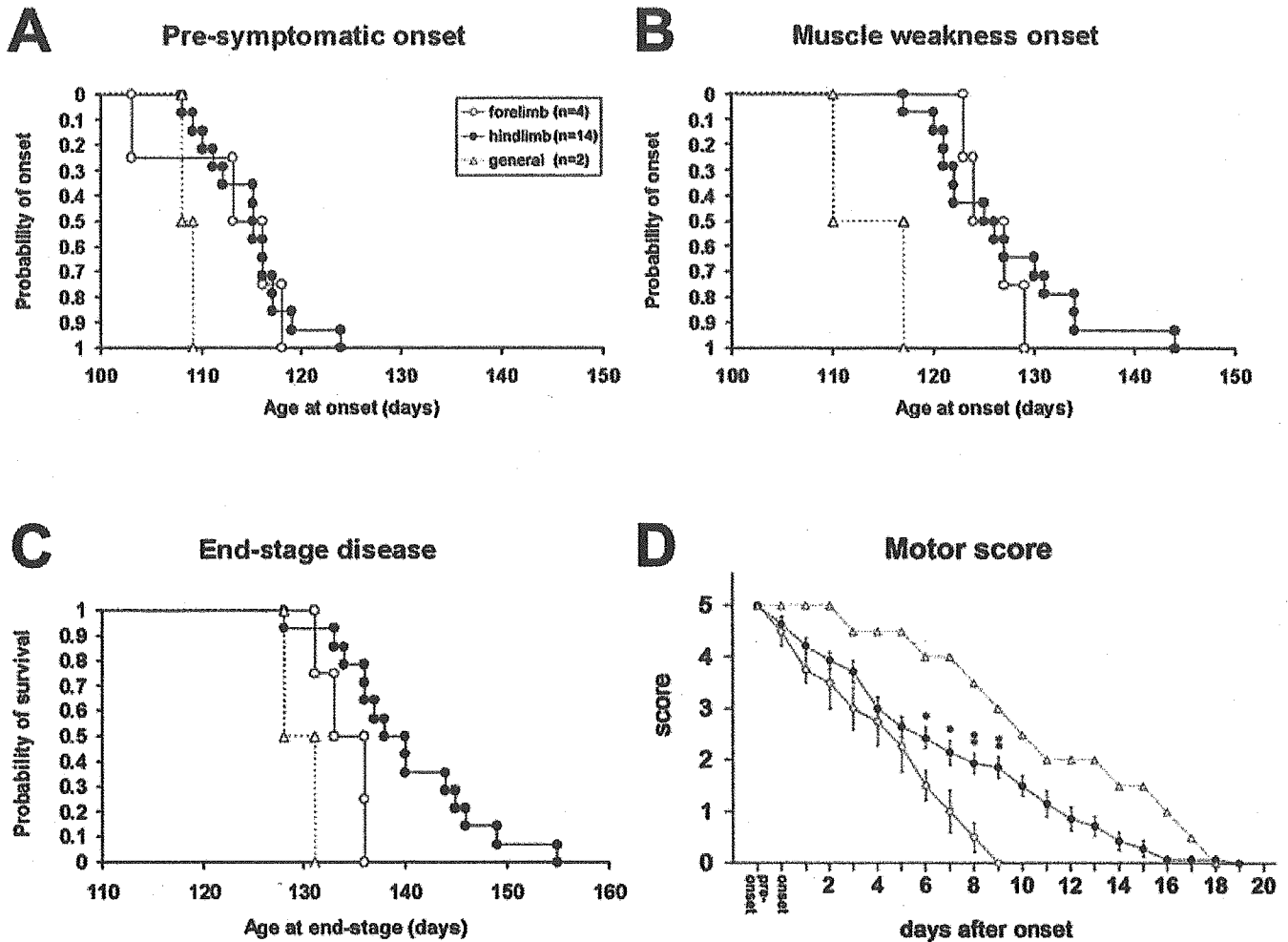


Fig. 5. Comparison of onset, end-stage, and disease progression in the forelimb-type ( $n = 4$ ), and the hindlimb-type ( $n = 14$ ) rats. Data from the general-type rats are also shown as dotted lines. **A,B:** The probability of the objective onsets. We did not see any differences in the probability of the objective onsets defined by body weight measurement (pre-symptomatic onset) and the inclined plane test (muscle weakness onset) between the forelimb- and hindlimb-type rats. **C:** The probability of survival as defined by end-stage disease. Survival was significantly shorter in the forelimb-type than in the hind-

limb-type rats ( $P < 0.05$ , Log-rank test). **D:** Assessment of disease progression using the Motor score. Affected rats were evaluated after muscle weakness onset. The forelimb type worsened more quickly than the hindlimb type. Score decline correlated well with the exacerbation of symptoms in both clinical types, clearly and objectively. Bars = means  $\pm$  SEM. Statistically significant differences between forelimb and hindlimb types are indicated in the figures. \* $P < 0.05$ . \*\* $P < 0.01$ ; two-tailed unpaired Student's  $t$ -test.

onsets (pre-symptomatic onset and muscle weakness onset), the probability of survival defined by end-stage disease (failure in righting reflex), and the Motor score (Table V, Fig. 5). We did not see any differences in the objective onsets between the forelimb- and hindlimb-type rats (Fig. 5AB, Table V). However, survival as defined by end-stage disease was significantly shorter in the forelimb-type than in the hindlimb-type rats ( $P < 0.05$ , Log-rank test, Fig. 5C). Moreover, the duration of the disease calculated from the muscle weakness onset was also significantly shorter in the forelimb-type ( $8.3 \pm 1.0$  days) than in the hindlimb-type rats ( $13.4 \pm 3.0$  days) (see ED - b,  $P < 0.01$ , two-tailed unpaired Student's  $t$ -test, Table V).

The courses of functional deterioration evaluated by the Motor score after onset (muscle weakness onset) for each clinical type were well represented by the declines in their scores (Fig. 5D). The assessment by the Motor score also showed that disease progression in the forelimb type was more rapid than that in the hindlimb type (Fig. 5D).

Our results raise the question of why this variability in the disease course of each clinical type was observed. We speculated that there might be correlation between clinical type in G93A rats and the amount of locally expressed mutant hSOD1 (G93A) gene product. Therefore, we next investigated expression of the mutant hSOD1 gene in each segment of the spinal cord (cervical, thoracic, and lumbar) in the forelimb- and

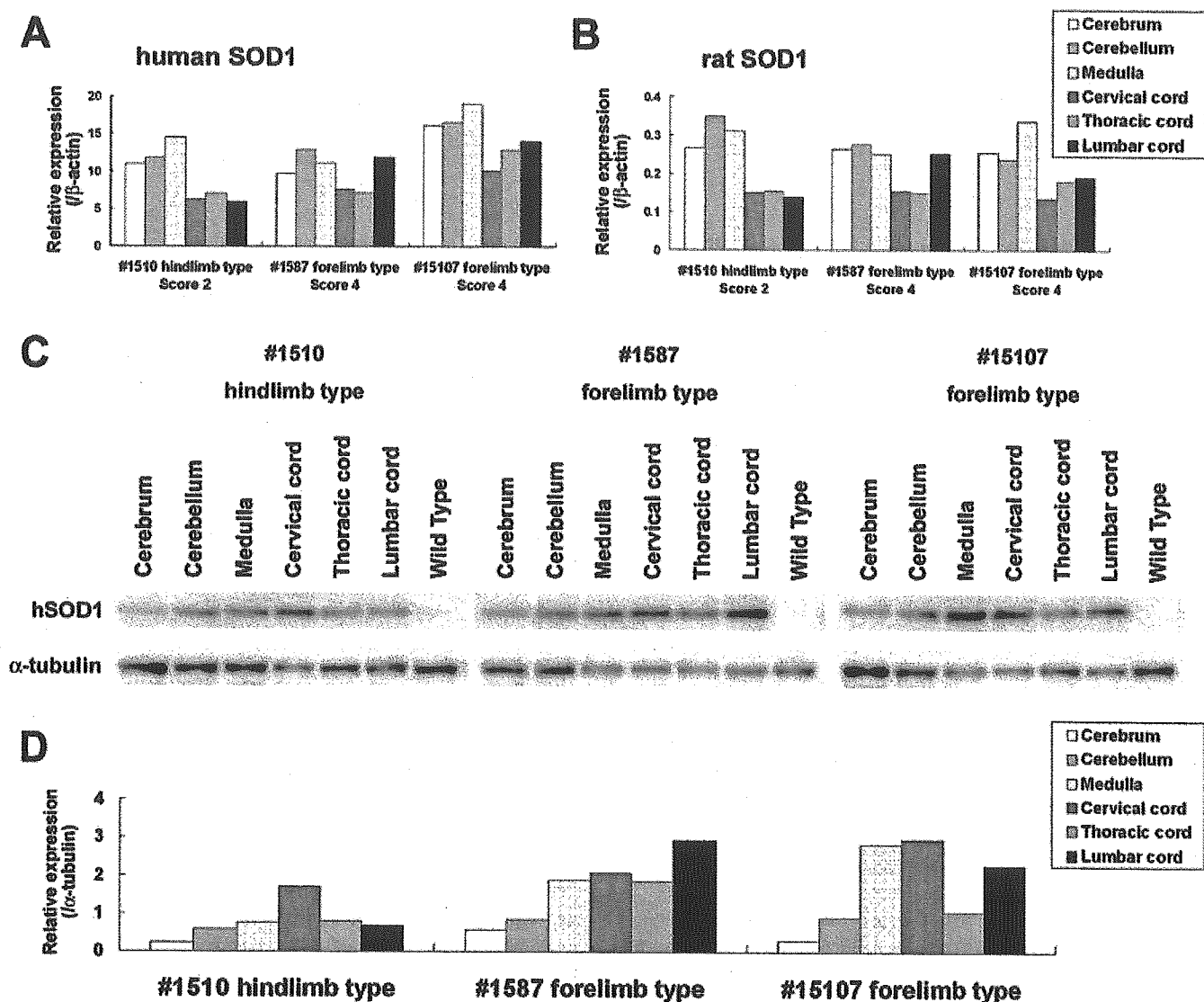


Fig. 6. The expression of mutant hSOD1 mRNA and protein in the cerebral cortex, cerebellum, medulla, and spinal cord (cervical, thoracic, and lumbar) of forelimb- and hindlimb-type rats. **A,B:** The amounts of human (A) and endogenous rat (B) SOD1 mRNA normalized to those of  $\beta$ -actin were quantified by real time RT-PCR analysis. **C,D:** Western blot analysis of the mutant hSOD1 protein was carried out in the same rats. Quantitative analysis was carried out with a Scion Image. The amounts of proteins were normalized to those of  $\alpha$ -tubulin (D).

hindlimb-type rats by real time RT-PCR and Western blot analysis. However, at least at the stages after the apparent onset of muscle weakness, neither forelimb-type (#1587, Score 4 and #15107, Score 4) nor hindlimb-type rats (#1510, Score 2) necessarily expressed larger amounts of the mutant hSOD1 (G93A) transgene in the cervical cord or in the lumbar cord, respectively, at the mRNA and the protein level (Fig. 6). We also investigated the expression of endogenous rat SOD1 mRNA in the same rats by REAL TIME RT-PCR (Fig. 6B). Distribution of endogenous rat SOD1 mRNA expressed in each segment of the spinal cord showed almost the same pattern as that of mutant

hSOD1 mRNA. The expression of endogenous rat SOD1 mRNA was lower than that of mutant hSOD1 mRNA. Thus, we could not detect any definite correlation between the hSOD1 (G93A) transgene local expression profile in the spinal cord and the phenotypes of G93A rats for either the forelimb-type or the hindlimb-type rats (Fig. 6).

#### Reduction in the Number of Spinal Cord Motor Neurons at Different Disease Stages

We examined histo-pathological changes in the spinal cords of the transgenic rats in comparison with those

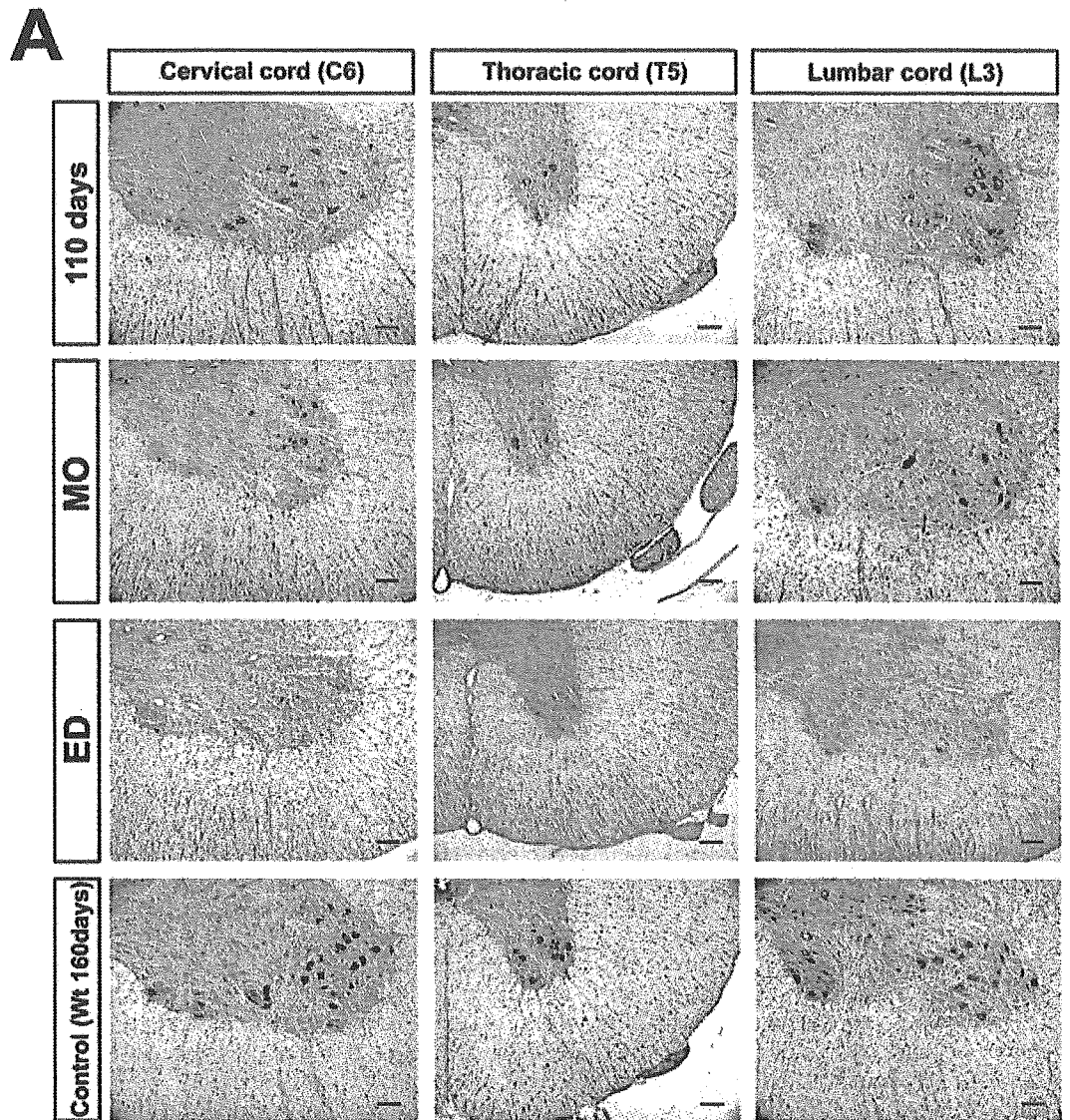
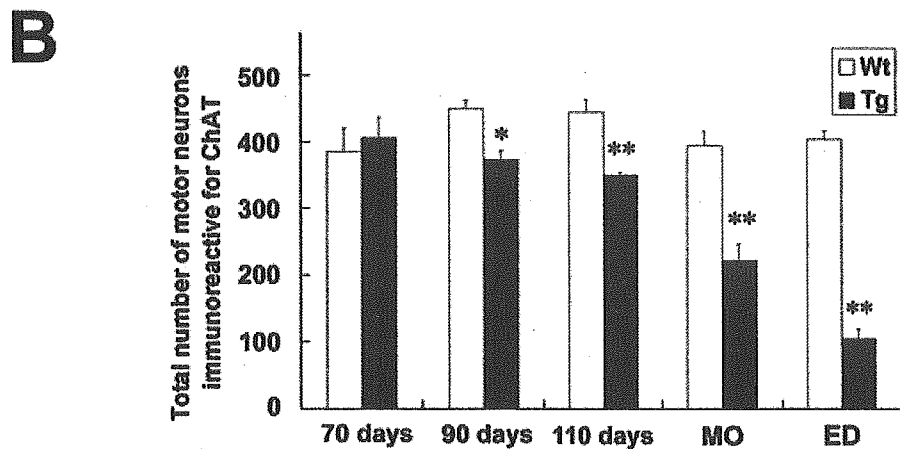


Fig. 7. The loss of motor neurons in the spinal cord of hSOD1 (G93A) transgenic rats at different stages. **A:** Immunohistochemical analysis of the spinal cord of transgenic rats. Transverse sections of the cervical (C6), thoracic (T5), and lumbar (L3) spinal cord of the transgenic rats and their wild-type littermates were stained with an anti-ChAT antibody to label viable motor neurons at the indicated stages (Scale bars = 100  $\mu$ m). **B:** The number of ChAT immunoreactive motor neurons was counted and is shown in the histograms as the total number of motor neurons in the C6, T5, and L3 segments. This number began to decrease in the transgenic rats at 90 days of age, rapidly declined after 110 days of age, and fell to about 50% and 25% of wild-type rats at the muscle weakness onset (MO, around 125 days) and at end-stage disease (ED, around 140 days), respectively. Bars = means  $\pm$  SEM ( $n = 3$  for each genotype). \* $P < 0.05$ . \*\* $P < 0.01$ ; two-tailed unpaired Student's  $t$ -test.



of their wild-type littermates at 70, 90, and 110 days of age, when the transgenic rats scored  $<70^\circ$  in the inclined plane test (muscle weakness onset), and failed the righting reflex. To quantify the number of spinal motor neurons, we stained spinal cord sections of both groups with an anti-ChAT antibody.

As shown in Figure 7A, the numbers of ChAT immunoreactive motor neurons in the cervical (C6), thoracic (T5), and lumbar (L3) segments of the spinal cord decreased with disease progression. Quantitative analysis of the residual motor neurons showed that the total number of motor neurons in the transgenic rats began to decrease at 90 days of age, rapidly declined after 110 days of age, and fell to about 50% and 25% of the numbers in age-matched wild-type littermates at the time the score was  $<70^\circ$  in the inclined plane test (muscle weakness onset) and of righting reflex failure, respectively (Fig. 7B).

## DISCUSSION

### Factors Underlying the Variability in Phenotypes of hSOD1 (G93A) Transgenic Rats

In previous studies of this G93A rat, only the hindlimb-type has been described, and the variety of phenotypes and variable clinical courses have not yet been mentioned (Nagai et al., 2001). Recently, however, another line of G93A rats backcrossed onto a Wistar background (SOD1<sup>G93A/HW<sup>r</sup></sup> rats) was reported to present two phenotypes, including forelimb-type, and a large inter-litter variability in disease onset (Storkebaum et al., 2005). In the same way, commonly used FALS model mice harboring hSOD1 (G93A) gene have been reported to have clinical variability to some extent, and some of them dominantly show forelimb paralysis (Gurney et al., 1994). In this study, we recognized various clinical types, including forelimb-, hindlimb-, and general-type and established quantitative methods to evaluate disease progression that can be applied to any of the clinical types of this ALS model. We have also shown the variability in disease progression to depend on clinical types, that is, disease progression after the onset was faster in forelimb-type than in hindlimb-type rats. This difference may be due to the aggressiveness of the disease per se because we evaluated the time point of "death" (end-stage disease) according to righting reflex failure (Howland et al., 2002) to exclude the influence of feeding problems (bulbar region) and respiratory failure (level C2–C4).

These findings give rise to the next question; why is this variety of phenotypes and variability in the clinical course observed in the same transgenic line? There are at least three possible explanations. One is that the variation is due to the heterogeneous genetic background of the Sprague-Dawley (SD) rat (i.e., the strain used to generate this transgenic line), which might have led to different phenotypes. This idea is supported by the fact that the SD strain shows a large inter-individual disease variability in other models of neurodegenerative disorders, such as

**TABLE VI. Adequacy of Evaluation Methods in Regard to Practical Use\***

	Body weight	Inclined plane	Cage activity	SCANET	Motor score
Objectivity	A	B	A	A	B
Sensitivity	A	B	C	(A)	-
Specificity	C	B	C	C	A
Motivation independence	A	B	B	D	B
Skill requirements	A	B	A	A	B
Cost of apparatus	B	B	D	D	A

\*A, more appropriate; B, appropriate; C, less appropriate; D, inappropriate.

Huntington's disease (Ouay et al., 2000). Similar phenotypic variability takes place in human FALS carrying the same mutations in hSOD1 gene (Abe et al., 1996; Watanabe et al., 1997; Kato et al., 2001), which could be explained by heterogeneous genetic backgrounds. Thus, the present transgenic ALS model rats may be highly useful to understand the mechanisms of bulbar onset, arm onset, or leg onset that are seen in human disease. There may be modifier genes of these phenotypes, which should be identified in the future study.

The second is that there is variability in the expression of the mutant hSOD1 protein. The transcriptional regulation of this exogenous gene could be affected by one or more unknown factors, such as epigenetic regulation, and may not be expressed uniformly throughout the spinal cord of each animal. Therefore, some rats might express mutant proteins more in the cervical spinal cord and others might express more in the lumbar cord, possibly resulting in the forelimb type and hindlimb type, respectively. However, we found no definite correlation between local expression levels of the mutant hSOD1 mRNA/protein in the spinal cord and the phenotypes of these animals, using real time RT-PCR and western blot analysis after the onset of muscle weakness, when the clinical type of the transgenic rats could be defined (Fig. 6). Moreover, the pathological analysis showed no correlation between the number of residual motor neurons in each segment and the phenotypes of end-stage animals. However, because  $>50\%$  of spinal motor neurons have already degenerated at the stage of muscle weakness onset, whether local expression of the mutant hSOD1 gene and segmental loss of motor neurons correlate with the clinical types of G93A rats should be further investigated by analyzing younger animals at a stage when motor neuron loss has not progressed as much.

The third explanation involves a structural property of the mutant hSOD1 (G93A) protein itself. It is now thought that mutations in the hSOD1 gene may alter the 3-D conformation of the enzyme and, in turn, result in the SOD1 protein acquiring toxic properties that cause ALS (Deng et al., 1993; Hand and Rouleau 2002). For instance, the hSOD1 (G93A) mutant protein has been reported to be susceptible to nonnative protein-protein interactions because of its mutation site and unfolded structure (Shipp et al., 2003; Furukawa and

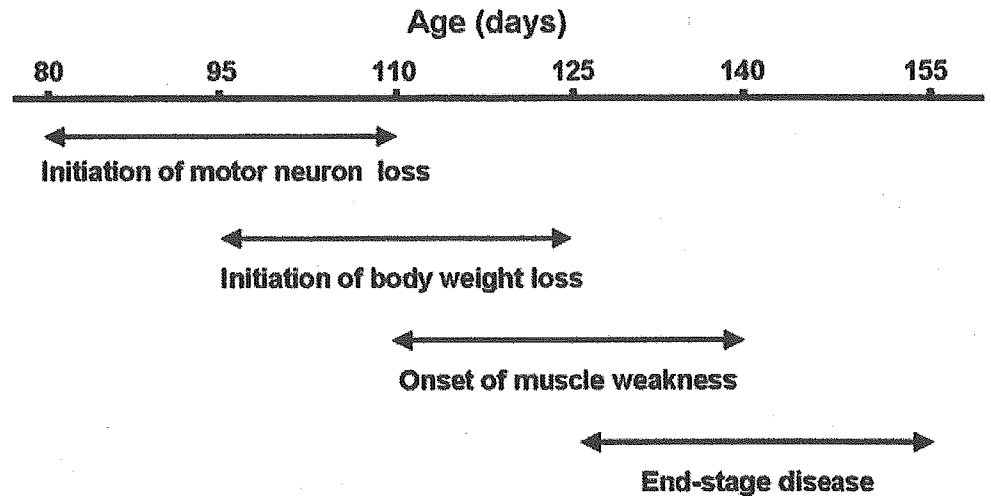


Fig. 8. Four stages of disease progression in hSOD1 (G93A) transgenic rats. The disease progression can be classified into four stages as shown. The range for each stage is about 1 month and overlaps approximately 2 weeks with the next stage.

O'Halloran, 2005), suggesting that the G93A mutation might accelerate the formation of SOD1 protein aggregates, which may ultimately sequester heat-shock proteins and molecular chaperones, disturb axonal transport or protein degradation machineries, including the ubiquitin-proteasome system (Borchelt et al., 1998; Bruening et al., 1999; Williamson and Cleveland 1999; Okado-Matsumoto and Fridovich 2002; Urushitani et al., 2002). Curiously, the mutated hSOD1 (G93A) protein is more susceptible to degradation by the ubiquitin-proteasome system and has a shorter half-life than other mutants (Fujiwara et al., 2005), suggesting that it may cause more unstable toxic aggregates in the spinal cord than other mutations. The degradation rate is also affected by environmental factors unique to each animal, such as the progressive decline of proteasome function with age (Keller et al., 2000), and these factors could contribute to the variability of the clinical course of G93A rats.

Taking all these findings into consideration, the mutated hSOD1 (G93A) protein may gain properties that are responsible for a variety of phenotypes and variability in the clinical course of the affected animals.

#### Characteristics of Different Methods for Assessing hSOD1 (G93A) Transgenic Rats

The ideal measure is not influenced by the judgment of the observer, sensitive to small abnormalities, specific to detect pathologic events that are related to pathogenesis of the ALS-like disease, not influenced by the motivational factors of rats, minimal in the requirements for skill in the observer, and inexpensive to carry out. We assessed each evaluation method by the categories in regard to practical use as shown in the Table 6.

The initiation of body weight loss seems to be an excellent marker to detect the onset and should be highly recommended. Muscle volume might have already started to decrease, even in the period of continuous weight gain, as reported for hSOD1 (G93A) transgenic mice (Brooks et al., 2004). As a result, it could detect an abnormality relatively earlier than subjective

onset. The inclined plane test is considered to be the least defective method of all. It could objectively and specifically detect the decline in the muscle strength of these ALS model rats as a muscle weakness onset almost at the same time of the subjective onset. The cage activity measurement and SCANET require very expensive apparatus, and are limited by the availability of funds and space for making the measurements. Although SCANET test was most sensitive among these measures, it seems inappropriate for the statistical analysis, and does not add any more information than that obtained through simple observation of the rats because the performances of the rats might be severely affected by the extent of their motivation to explore. Motor score can specifically assess disease progression of each clinical type and is valuable in keeping the experimental costs at a minimum.

#### Correlation Between the Loss of Spinal Motor Neurons and Disease Stages

This study clearly shows the variable clinical course of G93A rats. According to our behavioral and histological analyses, we can divide the disease course of this transgenic model into four stages, whose durations have a range of about 1 month, as shown in Figure 8. Furthermore, we have established the pathological validity of the performance deficits detected by each measure of disease progression. "Initiation of motor neuron loss" was defined as a statistically significant decrease in the number of spinal motor neurons, which was found at around 90 days of age, but not 70 days of age (Fig. 7B). This coincides with, and seems to be sensitively detected by the marked difference in SCANET scores that begins at around 90 days of age (Fig. 3D–F). The "initiation of body weight loss" was usually detected at around 110 days of age as the peak body weight (pre-symptomatic onset,  $113.6 \pm 4.8$  days of age, range = 103–124, Table IV). This stage coincides with the initiation of a rapid decline in the number of motor neurons at around 110 days of age (Fig. 7B). "Onset of muscle weakness" was detected at around 125 days of age, as assessed by the



inclined plane test (muscle weakness onset,  $125.2 \pm 7.4$  days of age, range = 110–144, Table IV). This coincides with the number of spinal motor neurons in the transgenic rats being reduced to about 50% of the number in wild-type rats (Fig. 7B). We presume that transgenic rats do not present obvious muscle weakness until the number of motor neurons has been reduced to approximately half the number found in the healthy state. “End-stage disease” as defined by righting reflex failure was recorded at around 140 days of age ( $137.8 \pm 7.1$  days of age, range = 122–155, Table IV). At this stage, the affected rats had only about 25% of the spinal motor neurons of age- and gender-matched wild-type rats (Fig. 7B), and showed a generalized loss of motor activity. Thus, our findings allow us to estimate the extent of spinal motor neuron loss by evaluating the disease stage with the measures described in this study.

In summary, we have described the variable phenotypes of mutant hSOD1 (G93A) transgenic rats and established an evaluation system applicable to all clinical types of these rats. Disease stages defined by this evaluation system correlated well pathologically with the reduction of motor neurons. Our evaluation system of this animal model should be a valuable tool for future preclinical experiments aimed at developing novel treatments for ALS.

#### ACKNOWLEDGMENTS

We thank Dr. H.-N. Dai of the Department of Neuroscience, Georgetown University School of Medicine for technical advice and valuable discussions, and Dr. T. Yoshizaki and Miss K. Kaneko for participating in the assessment of transgenic rats with the Motor score. This work was supported by grants from CREST, Japan Society for the Promotion of Science to H.O., a Research Grant on Measures for Intractable Diseases from the Japanese Ministry of Health, Labour and Welfare to H.O., M.A., G.S. and Y.I., and a Grant-in-Aid for the 21st century COE program to Keio University from the Japanese Ministry of Education, Culture, Sports, Science and Technology.

#### REFERENCES

- Abe K, Aoki M, Ikeda M, Watanabe M, Hirai S, Itoyama Y. 1996. Clinical characteristics of familial amyotrophic lateral sclerosis with Cu/Zn superoxide dismutase gene mutations. *J Neurol Sci* 136:108–116.
- Azzouz M, Ralph GS, Storkebaum E, Walmsley LE, Mitrophanous KA, Kingsman SM, Carmeliet P, Mazarakis ND. 2004. VEGF delivery with retrogradely transported lentivector prolongs survival in a mouse ALS model. *Nature* 429:413–417.
- Barneoud P, Lollivier J, Sanger DJ, Scatton B, Moser P. 1997. Quantitative motor assessment in FALS mice: a longitudinal study. *Neuroreport* 8:2861–2865.
- Borchelt DR, Wong PC, Becher MW, Pardo CA, Lee MK, Xu ZS, Thinakaran G, Jenkins NA, Copeland NG, Sisodia SS, Cleveland DW, Price DL, Hoffman PN. 1998. Axonal transport of mutant superoxide dismutase 1 and focal axonal abnormalities in the proximal axons of transgenic mice. *Neurobiol Dis* 5:27–35.
- Brooks KJ, Hill MD, Hockings PD, Reid DG. 2004. MRI detects early hindlimb muscle atrophy in Gly93Ala superoxide dismutase-1 (G93A SOD1) transgenic mice, an animal model of familial amyotrophic lateral sclerosis. *NMR Biomed* 17:28–32.
- Brown RH Jr. 1995. Amyotrophic lateral sclerosis: recent insights from genetics and transgenic mice. *Cell* 80:687–692.
- Bruening W, Roy J, Giasson B, Figlewicz DA, Mushynski WE, Durham HD. 1999. Up-regulation of protein chaperones preserves viability of cells expressing toxic Cu/Zn-superoxide dismutase mutants associated with amyotrophic lateral sclerosis. *J Neurochem* 72:693–699.
- Chiu AY, Zhai P, Dal Canto MC, Peters TM, Kwon YW, Pratts SM, Gurney ME. 1995. Age-dependent penetrance of disease in a transgenic mouse model of familial amyotrophic lateral sclerosis. *Mol Cell Neurosci* 6:349–362.
- de Bellerocche J, Orrell R, King A. 1995. Familial amyotrophic lateral sclerosis/motor neurone disease (FALS): a review of current developments. *J Med Genet* 32:841–847.
- Deng HX, Hentati A, Tainer JA, Iqbal Z, Cayabyab A, Hung WY, Getzoff ED, Hu P, Herzfeldt B, Roos RP, Warner C, Deng G, Soriano E, Smyth C, Parge HE, Ahmed A, Roses AD, Hallewell RA, Pericak-Vance MA, Siddique T. 1993. Amyotrophic lateral sclerosis and structural defects in Cu, Zn superoxide dismutase. *Science* 261:1047–1051.
- Fujiwara N, Miyamoto Y, Ogasahara K, Takahashi M, Ikegami T, Takamiya R, Suzuki K, Taniguchi N. 2005. Different immunoreactivity against monoclonal antibodies between wild-type and mutant copper/zinc superoxide dismutase linked to amyotrophic lateral sclerosis. *J Biol Chem* 280:5061–5070.
- Furukawa Y, O'Halloran TV. 2005. Amyotrophic lateral sclerosis mutations have the greatest destabilizing effect on the Apo- and reduced form of SOD1, leading to unfolding and oxidative aggregation. *J Biol Chem* 280:17266–17274.
- Gale K, Kerasidis H, Wrathall JR. 1985. Spinal cord contusion in the rat: behavioral analysis of functional neurologic impairment. *Exp Neurol* 88:123–134.
- Garbuzova-Davis S, Willing AE, Milliken M, Saporta S, Zigova T, Cahill DW, Sanberg PR. 2002. Positive effect of transplantation of hNT neurons (NTERA 2/D1 cell-line) in a model of familial amyotrophic lateral sclerosis. *Exp Neurol* 174:169–180.
- Gurney ME, Pu H, Chiu AY, Dal Canto MC, Polchow CY, Alexander DD, Caliendo J, Hentati A, Kwon YW, Deng HX, Chen W, Zhai F, Sufit RL, Siddique T. 1994. Motor neuron degeneration in mice that express a human Cu,Zn superoxide dismutase mutation. *Science* 264:1772–1775.
- Hand CK, Rouleau GA. 2002. Familial amyotrophic lateral sclerosis. *Muscle Nerve* 25:135–159.
- Howland DS, Liu J, She Y, Goad B, Maragakis NJ, Kim B, Erickson J, Kulik J, DeVito L, Psaltis G, DeGennaro LJ, Cleveland DW, Rothstein JD. 2002. Focal loss of the glutamate transporter EAAT2 in a transgenic rat model of SOD1 mutant-mediated amyotrophic lateral sclerosis (ALS). *Proc Natl Acad Sci USA* 99:1604–1609.
- Inoue H, Tsukita K, Iwasato T, Suzuki Y, Tomioka M, Tateno M, Nagao M, Kawata A, Saito TC, Miura M, Misawa H, Itoharu S, Takahashi R. 2003. The crucial role of caspase-9 in the disease progression of a transgenic ALS mouse model. *EMBO J* 22:6665–6674.
- Kaspar BK, Llado J, Sherkat N, Rothstein JD, Gage FH. 2003. Retrograde viral delivery of IGF-1 prolongs survival in a mouse ALS model. *Science* 301:839–842.
- Kato M, Aoki M, Ohta M, Nagai M, Ishizaki F, Nakamura S, Itoyama Y. 2001. Marked reduction of the Cu/Zn superoxide dismutase polypeptide in a case of familial amyotrophic lateral sclerosis with the homozygous mutation. *Neurosci Lett* 312:165–168.
- Keller JN, Huang FF, Zhu H, Yu J, Ho YS, Kindy TS. 2000. Oxidative stress-associated impairment of proteasome activity during ischemia-reperfusion injury. *J Cereb Blood Flow Metab* 20:1467–1473.
- Landis JR, Koch GG. 1977. The measurement of observer agreement for categorical data. *Biometrics* 33:159–174.
- Mikami Y, Toda M, Watanabe M, Nakamura M, Toyama Y, Kawakami Y. 2002. A simple and reliable behavioral analysis of locomotor function after spinal cord injury in mice. Technical note. *J Neurosurg Spine* 97:142–147.

- Mulder DW, Kurland LT, Offord KP, Beard CM. 1986. Familial adult motor neuron disease: amyotrophic lateral sclerosis. *Neurology* 36:511-517.
- Nagai M, Aoki M, Miyoshi I, Kato M, Pasinelli P, Kasai N, Brown RH, Jr., Itoyama Y. 2001. Rats expressing human cytosolic copper-zinc superoxide dismutase transgenes with amyotrophic lateral sclerosis: associated mutations develop motor neuron disease. *J Neurosci* 21:9246-9254.
- Ohki-Hamazaki H, Sakai Y, Kamata K, Ogura H, Okuyama S, Watase K, Yamada K, Wada K. 1999. Functional properties of two bombesin-like peptide receptors revealed by the analysis of mice lacking neuromedin B receptor. *J Neurosci* 19:948-954.
- Okada Y, Shimazaki T, Sobue G, Okano H. 2004. Retinoic-acid-concentration-dependent acquisition of neural cell identity during in vitro differentiation of mouse embryonic stem cells. *Dev Biol* 275:124-142.
- Okado-Matsumoto A, Fridovich I. 2002. Amyotrophic lateral sclerosis: a proposed mechanism. *Proc Natl Acad Sci USA* 99:9010-9014.
- Ouay S, Bizat N, Altairac S, Menetrat H, Mittoux V, Conde F, Hantraye P, Brouillet E. 2000. Major strain differences in response to chronic systemic administration of the mitochondrial toxin 3-nitropropionic acid in rats: implications for neuroprotection studies. *Neuroscience* 97:521-530.
- Rivlin AS, Tator CH. 1977. Objective clinical assessment of motor function after experimental spinal cord injury in the rat. *J Neurosurg* 47:577-581.
- Rosen DR, Siddique T, Patterson D, Figlewicz DA, Sapp P, Hentati A, Donaldson D, Goto J, O'Regan JP, Deng HX, Rahmani Z, Krizus A, McKenna-Yasek D, Cayabyab A, Gasten SM, Berger R, Tanzi RE, Halperin JJ, Herzfeldt B, van den Bergh R, Hung WY, Bird T, Deng G, Mulder DW, Smyth C, Laing NG, Soriano E, Pericak-Vance MA, Haines J, Reuleau GA, Gusella JS, Horvitz HR, Brown RH Jr. 1993. Mutations in Cu/Zn superoxide dismutase gene are associated with familial amyotrophic lateral sclerosis. *Nature* 362:59-62.
- Shipp EL, Cantini F, Bertini I, Valentine JS, Banci L. 2003. Dynamic properties of the G93A mutant of copper-zinc superoxide dismutase as detected by NMR spectroscopy: implications for the pathology of familial amyotrophic lateral sclerosis. *Biochemistry* 42:1890-1899.
- Storkebaum E, Lambrechts D, Dewerchin M, Moreno-Murciano MP, Appelmans S, Oh H, Van Damme P, Rutten B, Man WY, De Mol M, Wyns S, Manka D, Vermeulen K, Van Den Bosch L, Mertens N, Schmitz C, Robberecht W, Conway EM, Collen D, Moons L, Carmeliet P. 2005. Treatment of motoneuron degeneration by intracerebroventricular delivery of VEGF in a rat model of ALS. *Nat Neurosci* 8:85-92.
- Sun W, Funakoshi H, Nakamura T. 2002. Overexpression of HGF retards disease progression and prolongs life span in a transgenic mouse model of ALS. *J Neurosci* 22:6537-6548.
- Urushitani M, Kurisu J, Tsukita K, Takahashi R. 2002. Proteasomal inhibition by misfolded mutant superoxide dismutase 1 induces selective motor neuron death in familial amyotrophic lateral sclerosis. *J Neurochem* 83:1030-1042.
- Wang LJ, Lu YY, Muramatsu S, Ikeguchi K, Fujimoto K, Okada T, Mizukami H, Matsushita T, Hanazono Y, Kume A, Nagatsu T, Ozawa K, Nakano I. 2002. Neuroprotective effects of glial cell line-derived neurotrophic factor mediated by an adeno-associated virus vector in a transgenic animal model of amyotrophic lateral sclerosis. *J Neurosci* 22:6920-6928.
- Watanabe M, Aoki M, Abe K, Shoji M, Iizuka T, Ikeda Y, Hirai S, Kurokawa K, Kato T, Sasaki H, Itoyama Y. 1997. A novel missense point mutation (S134N) of the Cu/Zn superoxide dismutase gene in a patient with familial motor neuron disease. *Hum Mutat* 9:69-71.
- Weydt P, Hong SY, Klot M, Moller T. 2003. Assessing disease onset and progression in the SOD1 mouse model of ALS. *Neuroreport* 14:1051-1054.
- Williamson TL, Cleveland DW. 1999. Slowing of axonal transport is a very early event in the toxicity of ALS-linked SOD1 mutants to motor neurons. *Nat Neurosci* 2:50-56.



## Underediting of GluR2 mRNA, a neuronal death inducing molecular change in sporadic ALS, does not occur in motor neurons in ALS1 or SBMA

Yukio Kawahara<sup>a,1</sup>, Hui Sun<sup>a</sup>, Kyoko Ito<sup>a</sup>, Takuto Hideyama<sup>a</sup>,  
Masashi Aoki<sup>b</sup>, Gen Sobue<sup>c</sup>, Shoji Tsuji<sup>a</sup>, Shin Kwak<sup>a,\*</sup>

<sup>a</sup> Department of Neurology, Graduate School of Medicine, The University of Tokyo,  
7-3-1 Hongo, Bunkyo-ku, Tokyo 113-8655, Japan

<sup>b</sup> Department of Neurology, Tohoku University Graduate School of Medicine, Sendai, Japan

<sup>c</sup> Department of Neurology, Nagoya University Graduate School of Medicine, Nagoya, Japan

Received 7 July 2005; accepted 13 September 2005

Available online 12 October 2005

### Abstract

Deficient RNA editing of the AMPA receptor subunit GluR2 at the Q/R site is a primary cause of neuronal death and recently has been reported to be a tightly linked etiological cause of motor neuron death in sporadic amyotrophic lateral sclerosis (ALS). We quantified the RNA editing efficiency of the GluR2 Q/R site in single motor neurons of rats transgenic for mutant human Cu/Zn-superoxide dismutase (SOD1) as well as patients with spinal and bulbar muscular atrophy (SBMA), and found that GluR2 mRNA was completely edited in all the motor neurons examined. It seems likely that the death cascade is different among the dying motor neurons in sporadic ALS, familial ALS with mutant SOD1 and SBMA. © 2005 Elsevier Ireland Ltd and the Japan Neuroscience Society. All rights reserved.

**Keywords:** ALS; SOD1; Spinal and bulbar muscular atrophy; Motor neuron; RNA editing; GluR2; AMPA receptor; Neuronal death

### 1. Introduction

Amyotrophic lateral sclerosis (ALS) is a progressive neurodegenerative disease with selective loss of both upper and lower motor neurons, and familial cases are rare. The etiology of sporadic ALS remains elusive but recently deficient RNA editing of AMPA receptor subunit GluR2 at the Q/R site is reported in motor neurons in ALS that occurs in a disease-specific and motor neuron-selective manner (Kawahara et al., 2004; Kwak and Kawahara, 2005). Moreover, underediting of the GluR2 Q/R site greatly increases the Ca<sup>2+</sup> permeability of AMPA receptors (Hume et al., 1991; Verdoorn et al., 1991; Burnashev et al., 1992), which may cause neuronal death due to increased Ca<sup>2+</sup> influx through the receptor channel, hence mice with RNA editing deficiencies at the GluR2 Q/R site die young (Brusa et al., 1995) and mice transgenic for an artificial Ca<sup>2+</sup>-

permeable GluR2 develop motor neuron disease 12 months after birth (Kuner et al., 2005). Such evidence lends strong support to the close relevance of deficient RNA editing of the GluR2 at the Q/R site to death of motor neurons in sporadic ALS. However, although we and other researchers have demonstrated that dying neurons in several neurodegenerative diseases exhibit edited GluR2 (Kwak and Kawahara, 2005), it has not yet been demonstrated whether the underediting of GluR2 occurs in dying motor neurons in motor neuron diseases other than ALS. Such investigation is of particular importance since it will help clarify whether the molecular mechanism of motor neurons death is common among various subtypes of motor neurons.

ALS associated with the SOD1 mutation (ALS1) is the most frequent familial ALS (Rosen et al., 1993), and mutated human SOD1 transgenic animals have been studied extensively as a disease model of ALS1, yet the etiology of neuronal death in the animals has not been elucidated. Another example of non-ALS motor neuron disease is spinal and bulbar muscular atrophy (SBMA), which predominantly affects lower motor neurons with a relatively slow clinical course. Since the CAG

\* Corresponding author. Tel.: +81 3 5800 8672; fax: +81 3 5800 6548.

E-mail address: [kwak-tyk@umin.ac.jp](mailto:kwak-tyk@umin.ac.jp) (S. Kwak).

<sup>1</sup> Present address: The Wistar Institute, Philadelphia, PA, USA.

Table 1  
RNA editing efficiency of single motor neurons in SBMA

Case	Age at death (year)	Sex	No. of CAG repeats <sup>a</sup>	Postmortem delay (h)	GluR2(+) MN <sup>b</sup>	MN with 100% editing efficiency (% of GluR2(+) MN)
SBMA, case 1	71	M	48	2.5	12	12 (100)
SBMA, case 2	78	M	42	2.5	16	16 (100)
SBMA, case 3	60	M	44	1	16	16 (100)

<sup>a</sup> Number of CAG repeats in the androgen receptor gene.

<sup>b</sup> Motor neurons in which GluR2 RT-PCR amplifying product was detected.

repeat expansion in the androgen receptor gene has been demonstrated in SBMA (La Spada et al., 1991), and pharmacological castration is therapeutically effective in animal models (Katsuno et al., 2002, 2003), the death cascade responsible for SBMA is likely different from sporadic ALS. In this paper, an investigation is carried out into whether or not the dying mechanism underlying sporadic ALS is the same as ALS1 and SBMA by determining the editing status of the GluR2 Q/R site in single motor neurons.

## 2. Materials and methods

The animals used in this study were SOD1<sup>G93A</sup> and SOD1<sup>H46R</sup> transgenic male rats (Nagai et al., 2001) ( $n = 3$  each) that had exhibited progressive neuromuscular weakness with their littermates as the control ( $n = 3$  each) (Table 2). The first sign of disease in these rats was weakness of their hindlimbs, mostly exhibited by the dragging of one limb. Onset of motor neuron disease was scored as the first observation of abnormal gait or evidence of limb weakness. The mean age of onset of clinical weakness for the SOD1<sup>G93A</sup> and SOD1<sup>H46R</sup> lines was  $122.9 \pm 14.1$  and  $144.7 \pm 6.4$  days, respectively. As the disease progressed, the rats exhibited marked muscle wasting in their hindlimbs, and then in the forelimbs. The mean duration after the clinical expression of the disease in the SOD1<sup>G93A</sup> and SOD1<sup>H46R</sup> lines was  $8.3 \pm 0.7$  and  $24.2 \pm 2.9$  days, respectively (Nagai et al., 2001). The rats were killed 3 days and 2 weeks after the onset for the SOD1<sup>G93A</sup> and SOD1<sup>H46R</sup> lines, respectively, and we examined their fifth lumbar cord. Animals were handled according to Institutional Animal Care and Use Committee approved protocols that are in line with the Guideline for Animal Care and Use by the National Institute of Health. Spinal cords were isolated after deep pentobarbiturate anesthesia. In addition, spinal cords were obtained at autopsy from three genetically confirmed patients with SBMA (Table 1). Written informed consent was obtained from all subjects prior to death or from their relatives, and the Ethics Committees of Graduate School of Medicine, the University of Nagoya and the University of Tokyo approved the experimental procedures used. Spinal cords were rapidly frozen on dry ice and maintained at  $-80^\circ\text{C}$  until use.

Table 2  
RNA editing efficiency of single motor neurons in mutated human SOD1 transgenic rats

Case (n)	GluR2(+) MN <sup>a</sup>	MN with 100% editing efficiency (% of GluR2(+) MN)
SOD1 <sup>G93A</sup> -1	13	13 (100)
SOD1 <sup>G93A</sup> -2	21	21 (100)
SOD1 <sup>G93A</sup> -3	21	21 (100)
SOD1 <sup>H46R</sup> -1	19	19 (100)
SOD1 <sup>H46R</sup> -2	23	23 (100)
SOD1 <sup>H46R</sup> -3	20	20 (100)
SOD1 <sup>G93A</sup> , littermates (3)	22	22 (100)
SOD1 <sup>H46R</sup> , littermates (3)	20	20 (100)

<sup>a</sup> Motor neurons in which GluR2 RT-PCR amplifying product was detected.

Single motor neurons were isolated and collected into respective single test tubes that contained 200  $\mu\text{l}$  of TRIZOL Reagent (Invitrogen Corp., Carlsbad, CA, USA) using a laser microdissection system as previously described (Kawahara et al., 2003b, 2004) (LMD, Leica Microsystems Ltd., Germany) (Fig. 1a). After extracting total RNA from single neuron tissue, we analyzed the RNA editing efficiency at the GluR2 Q/R site by means of RT-PCR coupled with digestion of the PCR amplified products with a restriction enzyme Bbv-1 (New England BioLabs, Beverly, MA, USA) (Takuma et al., 1999; Kawahara et al., 2003a, 2004), and the editing efficiency was calculated by quantitatively analyzing the digests with a 2100 Bioanalyser (Agilent Technologies, Palo Alto, CA, USA), as previously described (Kawahara et al., 2003a). Briefly, after gel purification using ZymoClean Gel DNA Recovery Kit according to the manufacturer's protocol (Zymo Research, Orange, CA, USA), PCR products were quantified using a 2100 Bioanalyser. An aliquot (0.5  $\mu\text{g}$ ) was then incubated at  $37^\circ\text{C}$  for 12 h with  $10 \times$  restriction buffer and 2 U of Bbv-1 in a total volume of 20  $\mu\text{l}$  and inactivated at  $65^\circ\text{C}$  for 30 min. The PCR products had one intrinsic Bbv-1 recognition sites, whereas the products originating from unedited GluR2 mRNA had an additional recognition site. Thus, restriction digestion of the PCR products originating from edited rat (278 bp) and human (182 bp) GluR2 mRNA should produce two bands (human GluR2 in parenthesis) at 219 (116) and 59 (66) bp, whereas those originating from unedited GluR2 mRNA should produce three bands at 140 (81), 79 (35), and 59 (66) bp. As the 59 (66) bp band would originate from both edited and unedited mRNA, but the 219 (116) bp band would originate from only edited mRNA, we quantified the molarity of the 219 (116) and 59 (66) bp bands using the 2100 Bioanalyser and calculated the editing efficiency as the ratio of the former to the latter for each sample.

The following primers were used for PCR for rat and human GluR2 (amplified product lengths are also indicated): for rat GluR2 (278 bp): rF (5'-AGCAGATTTAGCCCTACGAG-3') and rR (5'-CAGCACTTTCGATGGGAGACAC-3'); for human GluR2, the first PCR (187 bp): hG2F1 (5'-TCTGGTTTTCCTGGGTGCC-3') and hG2R1 (5'-AGATCCTCAGCACTTTCG-3'); for the nested PCR (182 bp): hG2F2 (5'-GGTTTTCCTTG-GGTGCCCTTAT-3') and hG2R2 (5'-ATCCTCAGCACTTTCGATGG-3'). We confirmed that these primer pairs were situated in two distinct exons with an intron between them and did not amplify products originating from other GluR subunits (data not shown). PCR amplification for rat GluR2 was initiated with a denaturation step that was carried out at  $95^\circ\text{C}$  for 2 min, followed by 40 cycles of  $95^\circ\text{C}$  for 30 s,  $62^\circ\text{C}$  for 30 s, and  $72^\circ\text{C}$  for 1 min. PCR amplification for human GluR2 began with a 1 min denaturation step at  $95^\circ\text{C}$ , followed by 35 cycles of denaturation at  $95^\circ\text{C}$  for 10 s, annealing at  $64^\circ\text{C}$  for 30 s and extension at  $68^\circ\text{C}$  for 60 s. Nested PCR was conducted on 2  $\mu\text{l}$  of the first PCR product under the same conditions with the exception of the annealing temperature ( $66^\circ\text{C}$ ).

## 3. Results

The number of motor neurons was severely decreased in the spinal cord of SBMA patients, and we analyzed 44 neurons dissected from three cases (12 from case 1, 16 from cases 2 and 3). Restriction digestion of the PCR products yielded only 116 and 66 bp fragments but no 81 or 35 bp fragments as seen in ALS motor neurons in all the SBMA motor neurons examined. Likewise, restriction digestion of the PCR products from motor

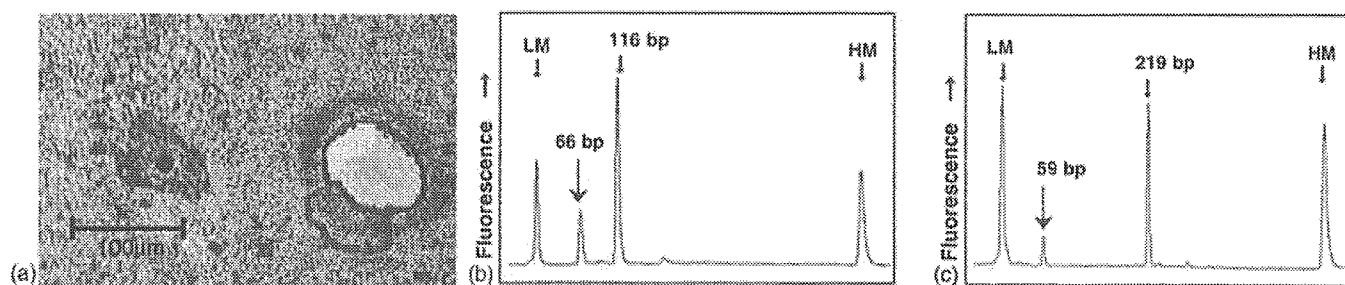


Fig. 1. (a) A single motor neuron from an SBMA patient before (left) and after (right) the dissection with a laser-microdissector. (b and c) An example of electropherogram by a 2100 Bioanalyser. Samples are the Bbv-I-digest of PCR product from tissues of a single motor neuron from an SBMA patient (b) and from a mutated human SOD1<sup>G93A</sup> transgenic mouse (c). LM: lower marker (15 bp). HM: higher marker (600 bp).

neurons of mutated human SOD1 transgenic rats yielded only 219 and 59 bp fragments (Fig. 1). Therefore, the values of RNA editing efficiency at the Q/R site of GluR2 were 100% in 44 motor neurons from three SBMA cases (Table 1), 55 single motor neurons from three SOD1<sup>G93A</sup> transgenic rats, 62 neurons from three SOD1<sup>H46R</sup> transgenic rats, as well as in 42 neurons from three littermate rats of each group (Table 2). The consistent finding that the GluR2 Q/R site is 100% edited in motor neurons of SBMA patients and transgenic rats for mutated human SOD1 is in marked contrast to the finding in ALS motor neurons that the editing efficiency widely varied among neurons ranging from 0% to 100% (Kawahara et al., 2004).

#### 4. Discussion

Compared to the significant underediting reported for the GluR2 Q/R site in motor neurons of sporadic ALS (Kawahara et al., 2004), GluR2 mRNA in all the examined motor neurons of the mutated human SOD1 transgenic rats with two different mutation sites and SBMA patients was completely edited at the Q/R site. We have confirmed that postmortem delay hardly influenced the editing efficiency at the GluR2 Q/R site (Kawahara et al., 2003b), hence the significant difference in the postmortem delay between the SBMA patients in this study and ALS patients in the previous report (Kawahara et al., 2004) would not have affected these results. We examined the motor neurons in the spinal cord segment corresponding to the hindlimb of mutated human SOD1 transgenic rats after their hindlimbs had become weak, indicating that the motor neurons examined were already pathologically affected. Likewise, we found that only a small number of motor neurons remained in the spinal cord of SBMA patients. Thus our results indicate that GluR2 RNA editing was complete in the dying motor neurons in both the mutated human SOD1 transgenic rats and SBMA patients, implying that the neuronal death mechanism is not due to the underediting of GluR2 mRNA seen in sporadic ALS. Since the pathogenic mechanism underlying ALS1 is considered to be the same as in mutant human SOD1 transgenic animals, motor neurons in affected ALS1 patients would be expected to have only edited GluR2 mRNA. Indeed, an association study of the SOD1 gene in a considerable number of patients with sporadic ALS reported no significant association with mutations of the SOD1 gene (Jackson et al., 1997). Due to

the lack of appropriate animal model for sporadic ALS, mutant human SOD1 transgenic animals have been used as a model for ALS in general, particularly in studies searching for therapeutically effective drugs. However, it should be kept in mind that mutated human SOD1 transgenic animals are merely a suggestive model for sporadic ALS and a gain of toxic function in mutated SOD1 kills motor neurons via mechanisms other than the demise of RNA editing. There are likely multiple different death pathways in motor neurons, and motor neurons in sporadic ALS, ALS1 and SBMA die by different death cascades.

#### Acknowledgements

This investigation was supported in part by grants-in-aid for Scientific Research on Priority Areas from the Ministry of Education, Culture, Sports, Science and Technology of Japan and grants from the Ministry of Health, Labor and Welfare of Japan (to SK), and a grant from Japan ALS Association (to YK).

#### References

- Brusa, R., Zimmermann, F., Koh, D., Feldmeyer, D., Gass, P., Seeburg, P., Sprengel, R., 1995. Early-onset epilepsy and postnatal lethality associated with an editing-deficient GluR-B allele in mice. *Science* 270, 1677–1680.
- Burnashev, N., Monyer, H., Seeburg, P., Sakmann, B., 1992. Divalent ion permeability of AMPA receptor channels is dominated by the edited form of a single subunit. *Neuron* 8, 189–198.
- Humé, R.I., Dingledine, R., Heinemann, S.F., 1991. Identification of a site in glutamate receptor subunits that controls calcium permeability. *Science* 253, 1028–1031.
- Jackson, M., Al-Chalabi, A., Enayat, Z.E., Chioza, B., Leigh, P.N., Morrison, K.E., 1997. Copper/zinc superoxide dismutase 1 and sporadic amyotrophic lateral sclerosis: analysis of 155 cases and identification of a novel insertion mutation. *Ann. Neurol.* 42, 803–807.
- Katsuno, M., Adachi, H., Doyu, M., Minamiyama, M., Sang, C., Kobayashi, Y., Inukai, A., Sobue, G., 2003. Leuprolin rescues polyglutamine-dependent phenotypes in a transgenic mouse model of spinal and bulbar muscular atrophy. *Nat. Med.* 9, 768–773.
- Katsuno, M., Adachi, H., Kume, A., Li, M., Nakagomi, Y., Niwa, H., Sang, C., Kobayashi, Y., Doyu, M., Sobue, G., 2002. Testosterone reduction prevents phenotypic expression in a transgenic mouse model of spinal and bulbar muscular atrophy. *Neuron* 35, 843–854.
- Kawahara, Y., Ito, K., Sun, H., Aizawa, H., Kanazawa, I., Kwak, S., 2004. RNA editing and death of motor neurons. *Nature* 427, 801.
- Kawahara, Y., Ito, K., Sun, H., Kanazawa, I., Kwak, S., 2003a. Low editing efficiency of GluR2 mRNA is associated with a low relative abundance of

- ADAR2 mRNA in white matter of normal human brain. *Eur. J. Neurosci.* 18, 23–33.
- Kawahara, Y., Kwak, S., Sun, H., Ito, K., Hashida, H., Aizawa, H., Jeong, S.-Y., Kanazawa, I., 2003b. Human spinal motoneurons express low relative abundance of GluR2 mRNA: an implication for excitotoxicity in ALS. *J. Neurochem.* 85, 680–689.
- Kuner, R., Groom, A.J., Bresink, I., Kornau, H.C., Stefovskaja, V., Muller, G., Hartmann, B., Tschauner, K., Waibel, S., Ludolph, A.C., Ikonomidou, C., Seeburg, P.H., Turski, L., 2005. Late-onset motoneuron disease caused by a functionally modified AMPA receptor subunit. *Proc. Natl. Acad. Sci. U.S.A.* 102, 5826–5831.
- Kwak, S., Kawahara, Y., 2005. Deficient RNA editing of GluR2 and neuronal death in amyotrophic lateral sclerosis. *J. Mol. Med.* 83, 110–120.
- La Spada, A.R., Wilson, E.M., Lubahn, D.B., Harding, A.E., Fischbeck, K.H., 1991. Androgen receptor gene mutations in X-linked spinal and bulbar muscular atrophy. *Nature* 352, 77–79.
- Nagai, M., Aoki, M., Miyoshi, I., Kato, M., Pasinelli, P., Kasai, N., Brown Jr., R.H., Itoyama, Y., 2001. Rats expressing human cytosolic copper–zinc superoxide dismutase transgenes with amyotrophic lateral sclerosis: associated mutations develop motor neuron disease. *J. Neurosci.* 21, 9246–9254.
- Rosen, D.R., Siddique, T., Patterson, D., Figlewicz, D.A., Sapp, P., Hentati, A., Donaldson, D., Goto, J., O'Regan, J.P., Deng, H.X., et al., 1993. Mutations in Cu/Zn superoxide dismutase gene are associated with familial amyotrophic lateral sclerosis. *Nature* 362, 59–62.
- Takuma, H., Kwak, S., Yoshizawa, T., Kanazawa, I., 1999. Reduction of GluR2 RNA editing, a molecular change that increases calcium influx through AMPA receptors, selective in the spinal ventral gray of patients with amyotrophic lateral sclerosis. *Ann. Neurol.* 46, 806–815.
- Verdoorn, T., Burnashev, N., Monye, R.H., Seeburg, P., Sakmann, B., 1991. Structural determinants of ion flow through recombinant glutamate receptor channels. *Science* 252, 1715–1718.

# Pharmacological induction of heat-shock proteins alleviates polyglutamine-mediated motor neuron disease

Masahisa Katsuno, Chen Sang, Hiroaki Adachi, Makoto Minamiyama, Masahiro Waza, Fumiaki Tanaka, Manabu Doyu, and Gen Sobue\*

Department of Neurology, Nagoya University Graduate School of Medicine, 65 Tsurumai-cho, Showa-ku, Nagoya 466-8550, Japan

Edited by L. L. Iversen, University of Oxford, Oxford, United Kingdom, and approved September 29, 2005 (received for review July 22, 2005)

Spinal and bulbar muscular atrophy (SBMA) is an adult-onset motor neuron disease caused by the expansion of a trinucleotide CAG repeat encoding the polyglutamine tract in the first exon of the androgen receptor gene (AR). The pathogenic, polyglutamine-expanded AR protein accumulates in the cell nucleus in a ligand-dependent manner and inhibits transcription by interfering with transcriptional factors and coactivators. Heat-shock proteins (HSPs) are stress-induced chaperones that facilitate the refolding and, thus, the degradation of abnormal proteins. Geranylgeranylacetone (GGA), a nontoxic antiulcer drug, has been shown to potently induce HSP expression in various tissues, including the central nervous system. In a cell model of SBMA, GGA increased the levels of Hsp70, Hsp90, and Hsp105 and inhibited cell death and the accumulation of pathogenic AR. Oral administration of GGA also up-regulated the expression of HSPs in the central nervous system of SBMA-transgenic mice and suppressed nuclear accumulation of the pathogenic AR protein, resulting in amelioration of polyglutamine-dependent neuromuscular phenotypes. These observations suggest that, although a high dose appears to be needed for clinical effects, oral GGA administration is a safe and promising therapeutic candidate for polyglutamine-mediated neurodegenerative diseases, including SBMA.

spinal and bulbar muscular atrophy | geranylgeranylacetone | androgen receptor | heat-shock factor-1

Expansion of a trinucleotide CAG repeat encoding the polyglutamine tract causes inherited neurodegenerative disorders, including spinal and bulbar muscular atrophy (SBMA), Huntington's disease, dentatorubral pallidoluysian atrophy, and several forms of spinocerebellar ataxia (1, 2). All these polyglutamine diseases show progressive and refractory neurological symptoms with selective neuronal cell loss within the susceptible regions of the nervous system. SBMA is a lower motor neuron disease exclusively affecting males and characterized by adult-onset proximal muscle atrophy, weakness, fasciculations, and bulbar involvement (3, 4). The molecular basis of this disease is elongation of a polyglutamine tract in the androgen receptor (AR) protein (5), the toxicity of which is considered a major cause of neurodegeneration in SBMA (6, 7). It has been postulated that pathogenesis in SBMA results from testosterone-dependent accumulation of pathogenic, polyglutamine-expanded AR in the cell nucleus (8, 9). This hypothesis is strongly supported by the observation that intranuclear accumulation of disease-causing protein leads to transcriptional dysregulation, a supposed pathway of neurodegeneration in polyglutamine diseases (10, 11).

Accumulated polyglutamine-containing protein is commonly seen as diffuse nuclear staining or as inclusion bodies, the histopathological hallmarks of polyglutamine diseases. Although inclusion bodies appear to represent a cellular defensive response, diffusely accumulated polyglutamine-containing protein in the nucleus possesses a distinctly toxic property (12–14). Accumulation of pathogenic protein is, thus, a major target of therapeutic

strategies for polyglutamine diseases. This view is supported by animal studies showing that hormonal interventions lowering serum testosterone levels successfully prevents nuclear accumulation of pathogenic AR and, thereby, rescue the phenotypes of mouse models of SBMA (8, 15, 16).

Heat-shock proteins (HSPs) are stress-induced molecular chaperones that play a crucial role in maintaining correct folding, assembly, and intracellular transport of proteins (17, 18). Under toxic conditions, HSP synthesis is rapidly up-regulated and nonnative proteins are refolded. There is increasing evidence that HSPs abrogate polyglutamine toxicity by refolding and solubilizing pathogenic proteins (19–21). Overexpression of Hsp70, together with Hsp40, inhibits toxic accumulation of abnormal polyglutamine protein and suppresses cell death in a variety of cellular models of polyglutamine diseases including SBMA (22–24). Hsp70 has also been shown to facilitate proteasomal degradation of abnormal AR protein in a cell culture model of SBMA (25). The salutary effects of Hsp70 have been verified in studies by using mouse models of polyglutamine diseases (26, 27). However, clinical applications based on these studies have certain limitations because they used genetic overexpression of Hsp70.

Geranylgeranylacetone (GGA) is an acyclic isoprenoid compound with a retinoid skeleton that induces HSP synthesis in various tissues including the gastric mucosa, intestine, liver, myocardium, retina, and central nervous system (28–32). Oral administration of GGA rapidly up-regulates HSP expression in response to a variety of stresses, although this effect is weak under nonstress conditions (29). With an extremely low toxicity, this compound has been widely used as an oral antiulcer drug. The aim of the present study is to investigate whether oral GGA induces HSP expression and thereby suppresses polyglutamine toxicity in cell culture and mouse models of SBMA.

## Materials and Methods

**Adenovirus Vector.** Adenovirus vectors were constructed with the BD Adeno-X Expression system according to the manufacturer's protocol (Invitrogen). Briefly, truncated AR constructs containing GFP (24 CAG repeats, 215 N-terminal amino acids of AR) or 97 CAG repeats, and 442 N-terminal amino acids of AR (23) were cloned into the pShuttle vector between the NheI and XbaI sites. pShuttle vectors with truncated AR24 or AR97 were digested with I-CeuI and P1-SceI. After *in vitro* ligation, recombinant adenovirus vector constructs containing the respective transgenic fragments were used to transfect HEK293 cells, and the vectors were isolated

Conflict of interest statement: No conflicts declared.

This paper was submitted directly (Track II) to the PNAS office.

Freely available online through the PNAS open access option.

Abbreviations: SBMA, spinal and bulbar muscular atrophy; AR, androgen receptor; GGA, geranylgeranylacetone; HSP, heat-shock protein; HSF-1, heat-shock factor-1.

\*To whom correspondence should be addressed. E-mail: sobueg@med.nagoya-u.ac.jp.

© 2005 by The National Academy of Sciences of the USA

by using the freeze-thaw method. Finally, virus titer was determined by using the BD Adeno-X Rapid Titer kit (Invitrogen).

**Cell Culture.** The human neuroblastoma cell line (SH-SY5Y, American Type Culture Collection No. CRL-2266) was maintained with DMEM/F12 (Invitrogen) supplemented with 10% FCS. After neural differentiation in differentiation medium (DMEM/F12 supplemented with 5% FCS and 10  $\mu$ M retinoic acid) for 4 days, SH-SY5Y cells were infected with the recombinant adenovirus vectors containing truncated AR24 or AR97 at a multiplicity of infection of 20 for 1 h and then treated with GGA. At each time point (0, 2, 4, and 6 days) after infection, cells were fixed with 4% paraformaldehyde for 10 min at room temperature, counterstained with propidium iodide (Molecular Probes), and mounted in Gelvatol. A confocal laser scanning microscope (MRC1024, Bio-Rad) and a conventional fluorescent microscope were used to determine the degree of neuronal cell death and the presence of GFP-labeled AR24 or AR97 protein in diffuse nuclear aggregates or in inclusion bodies. Quantitative analyses were made from triplicate determinations. Duplicate slides were graded blindly in two independent trials as described in ref. 23.

**Immunocytochemistry.** Cells were fixed with 4% paraformaldehyde and incubated with an anti-HSF-1 (HSF-1, heat-shock factor-1) antibody (1:5,000, Stressgen, Victoria, Canada) and anti-rabbit Alexa Fluor 568 antibody (1:1,000, Molecular Probes), then counterstained with Hoechst 33342 (Molecular Probes).

**Animals.** AR-24Q and AR-97Q mice were generated by using the pCAGGS vector as described in 8 and 33. The mouse rotarod task was performed with an Economex rotarod (Columbus Instruments, Columbus, OH), and cage activity was measured with the AB system (Neuroscience, Tokyo) as described in ref. 34. Each cage contained three mice, which were subjected to a 12-h light/dark cycle. All animal experiments were approved by the Animal Care Committee of Nagoya University Graduate School of Medicine.

**GGA Treatment.** GGA was a gift from Eisai, Inc. (Tokyo). For treating cultured SH-SY5Y cells, GGA was dissolved in absolute ethanol supplemented with 0.2%  $\alpha$ -tocopherol, and ethanol with  $\alpha$ -tocopherol alone was used as vehicle. For oral administration to mice, GGA granules were mixed with powdered rodent chow at concentrations of 0.25%, 0.5%, 1%, and 2%. GGA was administered to mice from 6 weeks of age until the end of the analysis without withdrawal or dose reduction. All mice had unlimited access to food and water. Net consumption of GGA was determined based on the amount of food consumed in each cage.

**Western Blotting.** SH-SY5Y cells were lysed in CellLytic lysis buffer (Sigma-Aldrich) containing a protease inhibitor mixture (Roche Diagnostics). Mouse tissues were homogenized in buffer containing 50 mM Tris (pH 8.0), 150 mM NaCl, 1% Nonidet P-40, 0.5% deoxycholate, 0.1% SDS, and 1 mM 2-mercaptoethanol with 1 mM PMSF, and 6  $\mu$ g/ml aprotinin and then centrifuged at 2,500  $\times$  g for 15 min. To extract the nuclear and cytoplasmic fractions, mouse tissues were treated with NE-PER nuclear and cytoplasmic extraction reagents (Pierce); cultured cells were lysed in buffer containing 10 mM Tris-HCl (pH 7.4), 10 mM NaCl, 3 mM MgCl<sub>2</sub>, and 0.5% Nonidet P-40 and then suspended in buffer containing 50 mM Tris-HCl (pH 6.8), 2% SDS, 6% glycerol, and protease inhibitor mixture (Roche Diagnostics). Equal amounts of protein were separated by 5–20% SDS/PAGE and transferred to Hybond-P membranes (Amersham Pharmacia Biotech). Primary antibodies and concentrations were as follows: AR (H-280, 1:1,000, Santa Cruz Biotechnology) Hsp70 (1:1,000, Stressgen Biotechnologies, Victoria, Canada), Hsc70 (1:5,000, Stressgen Biotechnologies), Hsp25 (1:5,000, Stressgen Biotechnologies), Hsp40 (1:5,000, Stressgen Biotechnologies), Hsp60 (1:5,000, Stressgen Biotechnologies),

Grp78 (1:5,000, Stressgen Biotechnologies), Hsp90 (1:1,000, Stressgen Biotechnologies), Hsp105 (1:250, Novocastra Laboratories, Newcastle, U.K.), HSF-1 (1:5,000, Stressgen Biotechnologies), and thioredoxin (1:2,000, Redox Bioscience, Kyoto, Japan). Primary antibody binding was probed with horseradish peroxidase-conjugated secondary antibodies at a dilution of 1:5,000, and bands were detected by using immunoreaction enhance solution (Can Get Signal, Toyobo, Japan) and enhanced chemiluminescence (ECL Plus, Amersham Biosciences, which is now GE Healthcare). An LAS-3000 imaging system (Fuji) was used to produce digital images. Signal intensities of three independent blots were quantified with IMAGE GAUGE software version 4.22 (Fuji) and expressed in arbitrary units. Membranes were reprobed with anti- $\alpha$ -tubulin (1:5,000, Santa Cruz Biotechnology), or anti-histone H3 (1:500, Upstate Biotechnology, Lake Placid, NY) antibodies for normalization.

**Immunohistochemistry.** Mice anesthetized with ketamine-xylazine were perfused with 4% paraformaldehyde fixative in phosphate buffer (pH 7.4). Tissues were dissected, postfixed in 10% phosphate-buffered formalin, and processed for paraffin embedding. Sections to be stained with anti-polyglutamine antibody 1C2 were treated with formic acid for 5 min at room temperature; those to be incubated with anti-HSF-1 antibody were boiled in 10 mM citrate buffer for 15 min. Primary antibodies and dilutions were as follows: polyglutamine (1:20,000, Chemicon, Temecula, CA), Hsp70 (1:500, Stressgen Biotechnologies), and anti-HSF-1 (1:5,000, Stressgen Biotechnologies). Primary antibody binding was probed with a labeled polymer of secondary antibody as part of the Envision+ system containing horseradish peroxidase (DakoCytomation, Gostrup, Denmark). The number of 1C2-positive cells in the spinal cord and muscle were determined as described in ref. 27.

**Statistical Analyses.** We analyzed data by using the Kaplan–Meier and log-rank test for survival rate, ANOVA with Dunnett's post hoc test for multiple comparisons, and an unpaired *t* test from STATVIEW software version 5 (Hulinks, Tokyo).

## Results

**GGA Suppresses Polyglutamine Toxicity in Cellular Model of SBMA.** To test whether GGA suppresses cellular toxicity induced by expanded polyglutamine, we generated a cultured cell model of SBMA. Adenovirus vector-mediated expression of a truncated AR with 97 CAGs (tAR97Q) resulted in the formation of inclusion bodies in the nucleus and cytoplasm as well as eventual cell death in human neuroblastoma cell line SH-SY5Y, whereas expression of AR containing only 24 CAGs (tAR24Q) showed no such toxicity (Fig. 1*A* and *B*). GGA administration reduced neuronal cell death as detected by propidium iodide staining in the cells expressing tAR97Q, the strongest effect occurring at a dose of 10<sup>-9</sup> M (Fig. 1*B* and *C*). Although GGA failed to decrease the number of the cells containing inclusion bodies, Western blot analysis using an anti-AR N terminus antibody demonstrated that GGA significantly diminished the amount of a high-molecular-weight complex, which likely corresponds to oligomers of tAR97Q (Fig. 1*D* and *E*) (35). Thus, GGA treatment suppresses cytotoxicity caused by accumulation of AR with elongated polyglutamine without inhibiting inclusion body formation.

**GGA Induces HSPs in Cellular Model of SBMA.** To determine whether the GGA-mediated mitigation of polyglutamine toxicity is due to HSP expression, we determined HSP levels in the cell culture model of SBMA after GGA treatment. GGA up-regulated expression of Hsp70, Hsp90, and Hsp105 in the cells with tAR97Q but did not in those with tAR24Q (Fig. 2*A* and *B*). Cycloheximide treatment eliminated GGA-mediated HSP induction and suppression of cell death (Fig. 2*C* and *D*). Expression of Hsc70, a constitutively expressed HSP, was not increased by GGA treatment; no GGA-mediated up-regulation was detected for other HSPs tested, such as



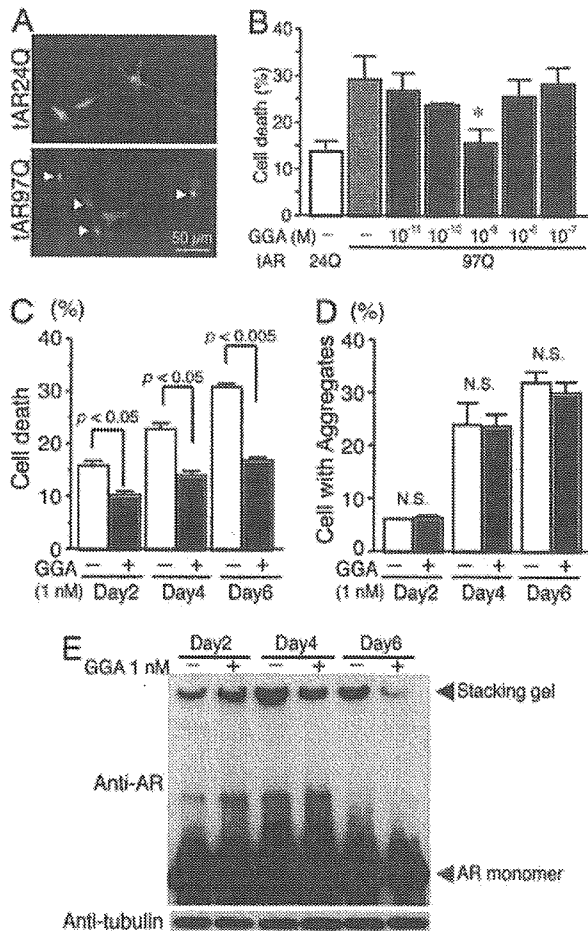


**Fig. 1.** Effects of GGA on polyglutamine toxicity in cultured cell. (A) Punctuated aggregates visualized with GFP (arrowhead) are formed in SHSY-5Y cells infected with an adenovirus vector containing truncated AR with 97 CAGs (tAR97Q-GFP) but not in those bearing tAR24Q. (B) Frequency of cell death 6 days after infection as detected by propidium iodine staining (\*,  $P < 0.05$  compared with untreated tAR97Q cells). (C) Suppression of cell death by GGA. (D) Frequency of cells bearing aggregates. (E) Anti-AR analysis of Western blots of extracts from cells infected with tAR97Q. Error bars indicate SD.

Hsp40 and Hsp60, or for thioredoxin, a redox-regulating protein (data not shown). Western blotting (Fig. 2E and F) and immunocytochemistry (Fig. 2G) revealed that GGA increased the nuclear uptake of hyperphosphorylated HSF-1, a transcription factor regulating HSP expression in the nucleus. Given that activated HSF-1 forms a hyperphosphorylated trimer and translocates into the nucleus, these findings suggest that GGA activates HSF-1, leading to HSP up-regulation.

**GGA Ameliorates Symptomatic Phenotypes of SBMA Mouse.** To examine whether pharmacological induction of HSPs alleviates polyglutamine-dependent neuronal dysfunction, oral GGA was administered to transgenic mice bearing human AR with 97 CAGs (AR-97Q). The actual amount of GGA was constant in each treatment group during the treatment period (see Table 1, which is published as supporting information on the PNAS web site). Oral GGA ameliorated muscle atrophy, gait disturbance, rotarod disability, and body weight loss in AR-97Q mice at both doses of 0.5 and 1% of food, which correspond to  $\approx 600$  and  $1,200 \text{ mg} \cdot \text{kg}^{-1} \cdot \text{day}^{-1}$ , respectively (Fig. 3A–E and Table 1). The life span of AR-97Q mice treated orally with 0.5 or 1% GGA was significantly extended compared with that of untreated AR-97Q mice. ( $P < 0.001$ ) (Fig. 3F). GGA failed to alleviate motor dysfunction in

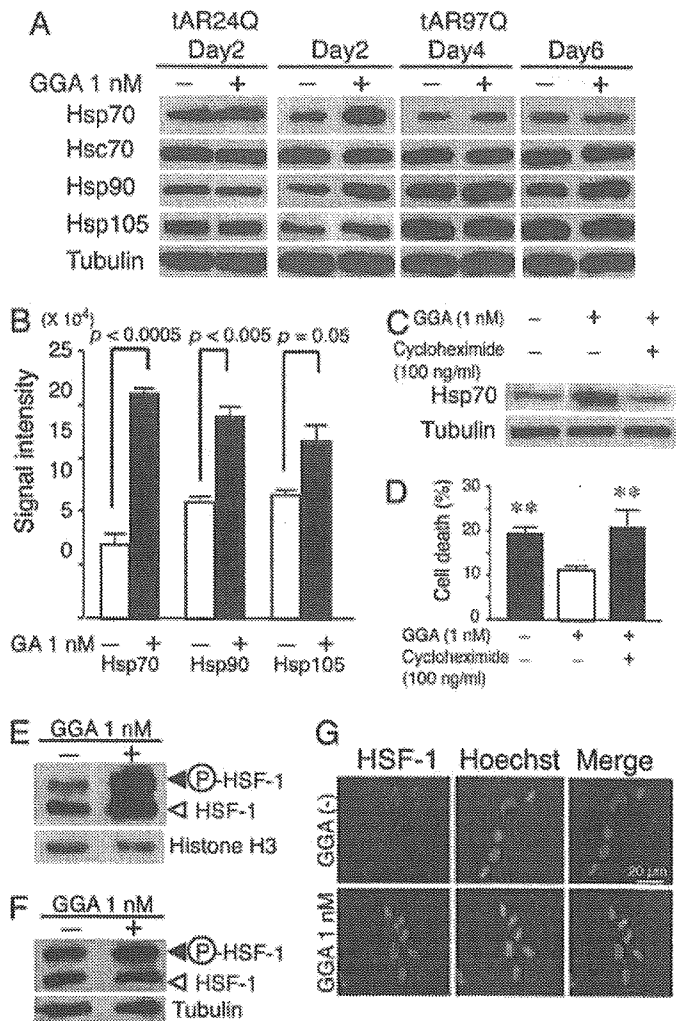


**Fig. 2.** GGA-mediated HSP induction in cultured cell. (A) Anti-HSP analysis of Western blots from cells infected with tAR97Q and treated with GGA. (B) Quantification of the levels of HSPs from tAR97Q-infected cells after 2 days of GGA treatment. (C) Anti-Hsp70 analysis of Western blots from tAR97Q cells treated with or without cycloheximide. (D) Frequency of cell death 2 days after infection as detected by propidium iodine staining (\*\*,  $P < 0.05$  compared with tAR97Q cells treated with GGA but not with cycloheximide). (E and F) Anti-HSF-1 analysis of Western blots of the cellular nuclear fraction (E) and that of total cell lysate (F). Upper bands correspond to the hyperphosphorylated, active form of HSF-1. (G) Immunocytochemistry for HSF-1. Error bars indicate SD.

AR-97Q mice at a dose of 0.25%. A higher dose of GGA, 2% of food, inhibited body growth and had no beneficial effects on the neurological phenotypes of the AR-97Q mice. Although no hepatic or renal toxicity was demonstrated at other doses, this high dose caused liver enlargement and dysfunction in wild-type and transgenic mice (see Table 2, which is published as supporting information on the PNAS web site).

**GGA Induces HSP Expression in SBMA Mice Through HSF-1 Activation.** To examine whether the GGA-induced improvement in the phenotypes of AR-97Q mice was due to induction of HSPs, the expression levels of HSPs were determined. Oral GGA increased the expression of Hsp70, Hsp90, and Hsp105 in the central nervous system and in the skeletal muscle of AR-97Q mice at the doses (0.5 and 1% of food) that were shown to improve symptomatic phenotypes of AR-97Q mice (Fig. 4A–C and Fig. 6A and B, which is published as supporting information on the PNAS web site). The

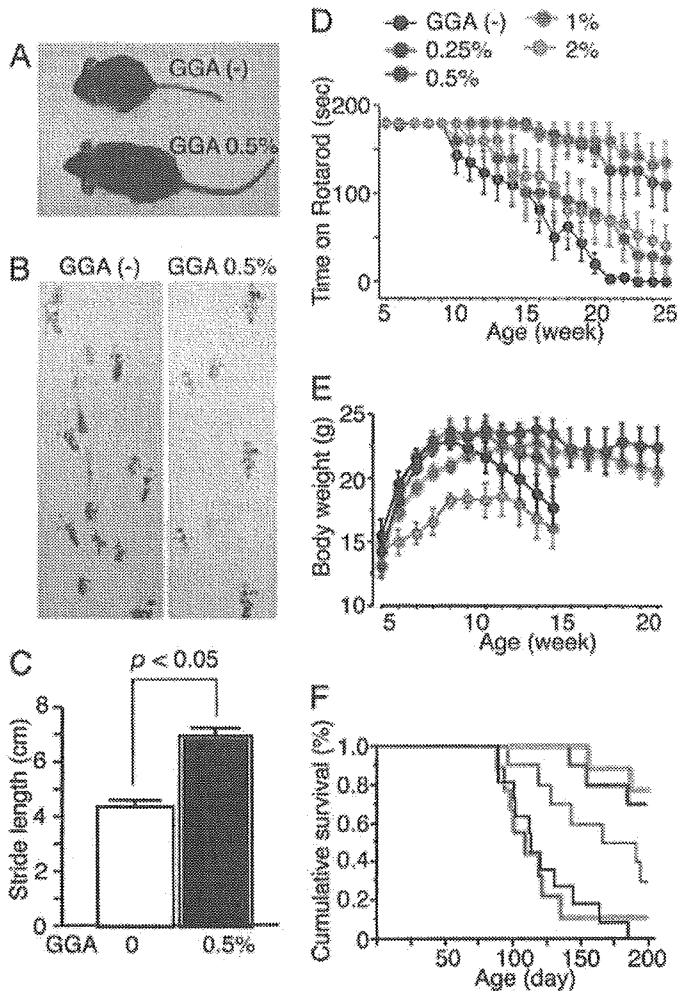


**Fig. 3.** Effect of GGA on neurological phenotypes of AR-97Q mice. (A) Muscle atrophy of 13-week AR-97Q mice. (B) Footprints of 13-week AR-97Q mice. Front paws are shown in red, and hind paws are shown in blue. (C) Stride distance of 13-week AR-97Q mice ( $n = 3$  for each group). (D–F) Rotarod task (D), body weight (E), and cumulative survival (F) of male AR-97Q mice treated with GGA ( $n = 12$  for each group) and untreated counterparts ( $n = 15$ ). Rotarod performance significantly improved after GGA at doses of 0.5% and 1.0% ( $P < 0.0001$  at both doses compared with nontreated mice at 20 weeks), and body weight increased significantly at a dose of 0.5% ( $P < 0.005$  at 0.5% and  $P < 0.05$  at 1.0%, at 14 weeks). Error bars indicate SD.

induction of HSPs was not clearly observed in the central nervous system until 3 weeks after treatment initiation, but it continued for at least 4 weeks thereafter (see Fig. 7A, which is published as supporting information on the PNAS web site). HSP induction by GGA was undetectable at a dose of 0.25% and was not significant at 2%, in agreement with the lack of therapeutic effect on motor function at these doses. Grp78, Hsp25, Hsp40, Hsp60, and thioredoxin were not induced by GGA administration (see Fig. 7B).

To examine whether GGA induced HSP expression through HSF-1 activation, the nuclear translocation of HSF-1 was investigated after GGA treatment. In the untreated state, the level of nuclear accumulated hyperphosphorylated HSF-1 in the central nervous systems of AR-97Q mice was lower than in the wild-type mice. However, when AR-97Q mice received 0.5% oral GGA, nuclear translocation of HSF-1 was higher than in the nontreated mice (Fig. 4D and Fig. 8, which is published as supporting information on the PNAS web site). In contrast, nuclear translocation of HSF-1 in skeletal muscle of untreated AR-97Q mice is already

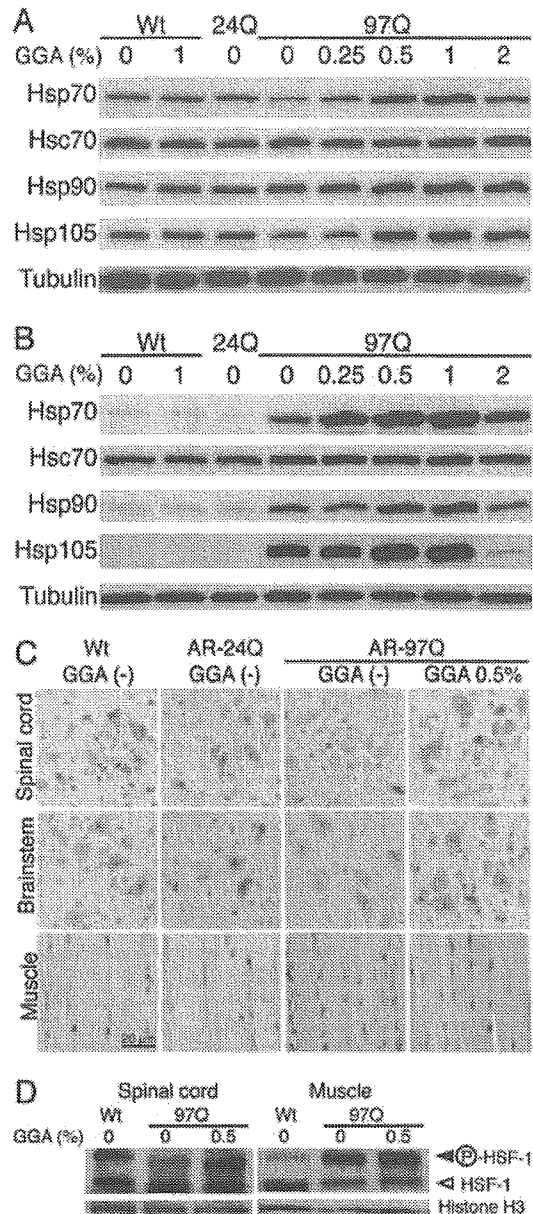


**Fig. 4.** GGA-mediated HSP induction in AR-97Q mice. (A) Western blotting for various HSPs in the spinal cord of 14-week, wild-type (Wt), AR-24Q and AR-97Q mice. (B) Western blotting for various HSPs in skeletal muscle of 14-week wild-type, AR-24Q, and AR-97Q mice. (C) Immunohistochemistry for Hsp70 in 14-week wild-type, AR-24Q, and AR-97Q mice. (D) Western blotting of nuclear fraction from spinal cord and that from muscle using anti-HSF-1 antibody. Upper bands correspond to the hyperphosphorylated active form of HSF-1.

much higher than in wild-type mice, thus perhaps explaining the high degree of Hsp70 induction in AR-97Q mice. After GGA treatment, nuclear translocation of HSF-1 in skeletal muscle of AR-97Q mice was even higher than it was in untreated AR-97Q mice, contributing to a higher induction of Hsp70 (Figs. 4D and 8). These experiments suggest that oral GGA restores activation of HSF-1, which is inhibited by expanded polyglutamine in the affected nervous tissues of AR-97Q mice.

**GGA Inhibits Accumulation of Pathogenic AR in Nucleus.** With the aim of evaluating the effect of GGA on the nuclear accumulation of abnormal AR, immunohistochemistry with anti-polyglutamine an-

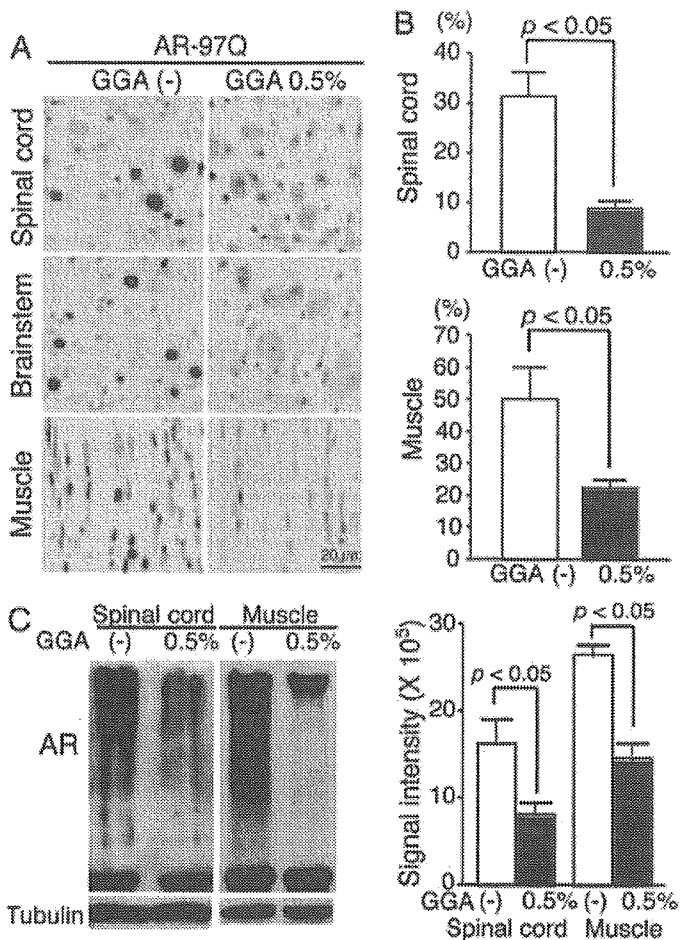


**Fig. 5.** Effect of GGA on accumulation of abnormal AR. (A) Immunohistochemistry of 14-week wild-type, AR-24Q, and AR-97Q mice using 1C2 antibody. (B) Quantification of 1C2-positive cells in spinal cord and muscle of AR-97Q mice treated with or without GGA. (C) Western blotting for AR of 14-week AR-97Q mice and quantification of the high-molecular-weight, abnormal AR complex indicated by a smear from the top of the gel. Error bars indicate 5D.

tibody 1C2 was performed on tissues from GGA-administrated and untreated AR-97Q mice. Oral 0.5% GGA decreased the number of 1C2-positive cells in nervous tissues and, to a lesser extent, in muscle (Fig. 5A and B). Western blot analysis using an antibody against AR demonstrated that 0.5% oral GGA reduced the amount of the high-molecular-weight complex of abnormal AR (Fig. 5C). These findings suggest that oral GGA-mediated HSP induction inhibits nuclear accumulation of abnormal AR, leading to mitigation of polyglutamine-dependent pathogenesis.

## Discussion

**GGA Induces HSP Expression.** In the present study, GGA induced Hsp70, Hsp90, and Hsp105 in a cultured cell model of SBMA, leading to abrogation of polyglutamine-mediated cytotoxicity. Furthermore, oral GGA alleviated neuronal dysfunction through induction of HSPs in SBMA mice.

GGA was first introduced as a nontoxic inducer of Hsp70 in rat gastric mucosa (28). Oral GGA has also been reported to induce Hsp70 in the central nervous system as well as in the small intestine, liver, heart, and retina of rodents without any adverse effects (29–32, 36, 37). The present study suggests that the required dose for HSP induction in the SBMA mouse model is  $\sim 600$  mg·kg<sup>-1</sup>·day<sup>-1</sup>, whereas 200 mg·kg<sup>-1</sup>·day<sup>-1</sup> induces HSP expression in nonneuronal tissues of rodents under stress (28, 36). Several

studies have verified that Hsp70 induction is due to GGA-mediated activation of HSF-1, a transcription factor that regulates expression of Hsp70 (28, 37). In the SBMA mice, GGA facilitated nuclear translocation of HSF-1, leading to induction of Hsp70, in the affected tissues.

GGA showed no adverse effects at the salutary doses used in the present study, although hepatic toxicity was detected at a higher dose. Low toxicity of GGA is advantageous, because continuous administration of GGA at a high dose is required for treating slowly progressive neurodegenerative disease (6, 7). Pharmacological induction of HSP by using GGA thus appears to be an applicable therapeutic strategy for SBMA, although careful attention should be paid to adverse effects during long-term treatment.

**HSPs as Therapeutics for Polyglutamine Diseases.** In the present study, GGA-mediated HSP induction resulted in inhibiting the accumulation of abnormal AR in the cellular and transgenic mouse models of SBMA. Accumulation of abnormal protein has been considered central to the pathogenesis of polyglutamine diseases, including SBMA. It has been postulated that expanded polyglutamine confers a monomeric protein conformational change from random coil to  $\beta$ -sheet, leading to formation of a polyglutamine oligomer (38, 39). The misfolded monomer and oligomer exercise their toxic effects by interacting with normal cellular proteins. Direct inhibition of polyglutamine oligomerization by Congo red has been demonstrated to exert therapeutic effects in a mouse model of Huntington's disease (40). Whereas oligomerization of causative proteins has been implicated in the pathogenic processes of neurodegeneration in polyglutamine diseases, the formation of inclusion bodies or mature amyloid fibrils appears to possess cytoprotective properties (13, 41). Based on this hypothesis, HSPs have been drawing a great deal of attention because they inhibit oligomer assembly and thereby mitigate polyglutamine toxicity (20, 21, 38). This view is supported by the fact that overexpression of Hsp70 attenuates the accumulation of polyglutamine-containing protein, resulting in amelioration of neurodegeneration in animal models of spinocerebellar ataxias or SBMA (26, 27).

GGA treatment significantly suppressed nuclear accumulation of abnormal AR in SBMA mice but did not inhibit inclusion body formation in cultured cells. This inconsistency does not necessarily deny a beneficial effect of GGA on polyglutamine aggregation, because it can be explained by several lines of evidence: (i) HSPs facilitate amyloid fibril formation by stabilizing the conformation of abnormal polyglutamine-expanded protein (42), and (ii) HSPs biochemically alter the structure of inclusion bodies (43, 44).

Hsp70 overexpression, however, fails to alleviate neurodegeneration or aggregate formation in the R6/2 mouse model of Huntington's disease (45, 46). This discord appears to indicate that higher levels of Hsp70 or the concomitant induction of other HSPs is required to alleviate Huntington's disease pathology. In addition to Hsp70, various molecular chaperones that colocalize with aggregates have also been shown to suppress polyglutamine toxicity: Hsp40-associated Hsp70 (23, 43), Hsp90, and Hsp105 (47, 48). Oral GGA induced Hsp90 and Hsp105 in the mouse model of SBMA and such diverse HSP up-regulation might contribute to the beneficial effects of GGA in the SBMA mice.

**HSP in Pathogenesis of polyQ Diseases.** Not only are HSPs considered potent suppressors of polyglutamine toxicity, but they are also implicated in the pathogenesis of neurodegeneration (20). There are several lines of evidence that polyglutamine elongation weakens the protective responses for coping with cellular stress. Truncated AR with expanded polyglutamine delays the induction of Hsp70 after heat shock (49). In the SBMA mice we examined, the level of Hsp70 in spinal cord was decreased before the onset of motor dysfunction. A similar finding has also been reported in the R6/2 mouse model of Huntington's disease (46).

In our SBMA mice, abnormal, polyglutamine-expanded AR seems to inhibit nuclear translocation of HSF-1 in the central nervous system, leading to a decrease in the level of Hsp70. In mammalian cells, induction of Hsp70 requires activation and nuclear localization of HSF-1. In the presence of nonnative protein, HSF-1 is derepressed, forming a trimer that translocates into the nucleus and binds to heat-shock elements within the gene encoding Hsp70 (50). In cellular models, this stress-induced nuclear accumulation of HSF-1 has been designated nuclear granules (51). Aggregates of abnormal ataxin-1, the causative protein in spinocerebellar ataxia 1, have been shown to hinder induction of nuclear granules in response to heat shock (52). Therefore, failure of HSF-1 activation appears to enhance polyglutamine toxicity. In this context, it is intriguing that inhibition of the nuclear accumulation of HSF-1 was detected in spinal cord but not in muscle of SBMA transgenic mice. Given that the threshold for HSP induction is relatively high in motor neurons (53), motor-neuron-specific inactivation of HSP transcription might partially explain why the central nervous system

is selectively affected in polyglutamine diseases including SBMA.

**HSP-Based Therapy for Neurodegeneration.** Both genetic and pharmacological manipulations of HSPs have been demonstrated to mitigate the pathogenesis of neurodegeneration (54–57). These observations suggest that GGA-mediated HSP induction may provide a therapeutic strategy for diverse neurodegenerative disorders, because these diseases share common pathogenic mechanisms such as abnormal protein aggregation, disruption of the ubiquitin-proteasome system and activation of the apoptotic pathway.

In summary, our observations indicate that GGA is a safe and promising therapeutic approach for treating many devastating neurodegenerative diseases, including SBMA.

We thank Eisai, Inc. for providing GGA. This work was supported by a Center-of-Excellence grant from the Ministry of Education, Culture, Sports, Science and Technology of Japan and grants from the Ministry of Health, Labor, and Welfare of Japan.

- Zoghbi, H. Y. & Orr, H. T. (2000) *Annu. Rev. Neurosci.* **23**, 217–247.
- Ross, C. A. (2002) *Neuron* **35**, 819–822.
- Kennedy, W. R., Alter, M. & Sung, J. H. (1968) *Neurology* **18**, 671–680.
- Sobue, G., Hashizume, Y., Mukai, E., Hirayama, M., Mituma, T. & Takahashi, A. (1989) *Brain* **112**, 209–232.
- La Spada, A. R., Wilson, E. M., Lubahn, D. B., Harding, A. E. & Fischbeck, K. H. (1991) *Nature* **352**, 77–79.
- Fischbeck, K. H., Lieberman, A., Bailey, C. K., Abel, A. & Merry, D. E. (1999) *Philos. Trans. R. Soc. London B* **354**, 1075–1078.
- Katsuno, M., Adachi, H., Tanaka, F. & Sobue, G. (2004) *J. Mol. Med.* **82**, 298–307.
- Katsuno, M., Adachi, H., Kume, A., Li, M., Nakagomi, Y., Niwa, H., Sang, C., Kobayashi, Y., Doyu, M. & Sobue, G. (2002) *Neuron* **35**, 843–854.
- Takeyama, K., Ito, S., Yamamoto, A., Tanimoto, H., Furutani, T., Kanuka, H., Miura, M., Tabata, T. & Kato, S. (2002) *Neuron* **35**, 855–864.
- Nucifora, F. C., Jr., Sasaki, M., Peters, M. F., Huang, H., Cooper, J. K., Yamada, M., Takahashi, H., Tsuji, S., Troncoso, J., Dawson, V. L., Dawson, T. M. & Ross, C. A. (2001) *Science* **291**, 2423–2428.
- Minamiyama, M., Katsuno, M., Adachi, H., Waza, M., Sang, C., Kobayashi, Y., Tanaka, F., Doyu, M., Inukai, A. & Sobue, G. (2004) *Hum. Mol. Genet.* **13**, 1183–1192.
- Yamada, M., Wood, J. D., Shimohata, T., Hayashi, S., Tsuji, S., Ross, C. A. & Takahashi, H. (2001) *Ann. Neurol.* **49**, 14–23.
- Arrasate, M., Mitra, S., Schweitzer, E. S., Segal, M. R. & Finkbeiner, S. (2004) *Nature* **431**, 805–810.
- Adachi, H., Katsuno, M., Minamiyama, M., Waza, M., Sang, C., Nakagomi, Y., Kobayashi, Y., Tanaka, F., Doyu, M. & Inukai, A., et al. (2005) *Brain* **128**, 659–670.
- Katsuno, M., Adachi, H., Doyu, M., Minamiyama, M., Sang, C., Kobayashi, Y., Inukai, A. & Sobue, G. (2003) *Nat. Med.* **9**, 768–773.
- Chevalier-Larsen, E. S., O'Brien, C. J., Wang, H., Jenkins, S. C., Holder, L., Lieberman, A. P. & Merry, D. E. (2004) *J. Neurosci.* **24**, 4778–4786.
- Welch, W. J. & Brown, C. R. (1996) *Cell Stress Chaperones* **1**, 109–115.
- Morimoto, R. I. & Santoro, M. G. (1998) *Nat. Biotechnol.* **16**, 833–838.
- Kobayashi, Y. & Sobue, G. (2001) *Brain Res. Bull.* **56**, 165–168.
- Wyttenbach, A. (2004) *J. Mol. Neurosci.* **23**, 69–96.
- Muchowski, P. J. & Wacker, J. L. (2005) *Nat. Rev. Neurosci.* **6**, 11–22.
- Cummings, C. J., Mancini, M. A., Antalfy, B., DeFranco, D. B., Orr, H. T. & Zoghbi, H. Y. (1998) *Nat. Genet.* **19**, 148–154.
- Kobayashi, Y., Kume, A., Li, M., Doyu, M., Hata, M., Ohtsuka, K. & Sobue, G. (2000) *J. Biol. Chem.* **275**, 8772–8778.
- Wyttenbach, A., Swartz, J., Kita, H., Thykjaer, T., Carmichael, J., Bradley, J., Brown, R., Maxwell, M., Schapira, A., Orntoft, T. F., et al. (2001) *Hum. Mol. Genet.* **10**, 1829–1845.
- Bailey, C. K., Andriola, I. F., Kampinga, H. H. & Merry, D. E. (2002) *Hum. Mol. Genet.* **11**, 515–523.
- Cummings, C. J., Sun, Y., Opal, P., Antalfy, B., Mestril, R., Orr, H. T., Dillmann, W. H. & Zoghbi, H. Y. (2001) *Hum. Mol. Genet.* **10**, 1511–1518.
- Adachi, H., Katsuno, M., Minamiyama, M., Sang, C., Pagoulatos, G., Angelidis, C., Kusakabe, M., Yoshiki, A., Kobayashi, Y., Doyu, M. & Sobue, G. (2003) *J. Neurosci.* **23**, 2203–2211.
- Hirakawa, T., Rokutan, K., Nikawa, T. & Kishi, K. (1996) *Gastroenterology* **111**, 345–357.
- Yamagami, K., Yamamoto, Y., Ishikawa, Y., Yonezawa, K., Toyokuni, S. & Yamaoka, Y. (2000) *J. Lab. Clin. Med.* **135**, 465–475.
- Ooie, T., Takahashi, N., Saikawa, T., Nawata, T., Arikawa, M., Yamanaka, K., Hara, M., Shimada, T. & Sakata, T. (2001) *Circulation* **104**, 1837–1843.
- Ishii, Y., Kwong, J. M. & Caprioli, J. (2003) *Invest. Ophthalmol. Vis. Sci.* **44**, 1982–1992.
- Fujiki, M., Kobayashi, H., Abe, T. & Ishii, K. (2003) *Brain Res.* **991**, 254–257.
- Niwa, H., Yamamura, K. & Miyazaki, J. (1991) *Gene* **108**, 193–199.
- Adachi, H., Kume, A., Li, M., Nakagomi, Y., Niwa, H., Do, J., Sang, C., Kobayashi, Y., Doyu, M. & Sobue, G. (2001) *Hum. Mol. Genet.* **10**, 1039–1048.
- Iuchi, S., Hoffner, G., Verbeke, P., Drijan, P. & Green, H. (2003) *Proc. Natl. Acad. Sci. USA* **100**, 2409–2414.
- Tsuruma, T., Yagihashi, A., Koide, S., Araya, J., Tarumi, K., Watanabe, N. & Hirata, K. (1999) *Transplant Proc.* **31**, 572–573.
- Yamanaka, K., Takahashi, N., Ooie, T., Kaneda, K., Yoshimatsu, H. & Saikawa, T. (2003) *J. Mol. Cell Cardiol.* **35**, 785–794.
- Sakahira, H., Breuer, P., Hayer-Hartl, M. K. & Hartl, F. U. (2002) *Proc. Natl. Acad. Sci. USA* **99**, 16412–16418.
- Perutz, M. F., Pope, B. J., Owen, D., Wanker, E. E. & Scherzinger, E. (2002) *Proc. Natl. Acad. Sci. USA* **99**, 5596–5600.
- Sanchez, I., Mahlke, C. & Yuan, J. (2003) *Nature* **421**, 373–379.
- Wacker, J. L., Zareie, M. H., Fong, H., Sarikaya, M. & Muchowski, P. J. (2004) *Nat. Struct. Mol. Biol.* **11**, 1215–1222.
- Hsu, A. L., Murphy, C. T. & Kenyon, C. (2003) *Science* **300**, 1142–1145.
- Muchowski, P. J., Schaffar, G., Sittler, A., Wanker, E. E., Hayer-Hartl, M. K. & Hartl, F. U. (2000) *Proc. Natl. Acad. Sci. USA* **97**, 7841–7846.
- Chan, H. Y., Warrick, J. M., Gray-Board, G. L., Paulson, H. L. & Bonini, N. M. (2000) *Hum. Mol. Genet.* **9**, 2811–2820.
- Hansson, O., Nylandsted, J., Castilho, R. F., Leist, M., Jaattela, M. & Brundin, P. (2003) *Brain Res.* **970**, 47–57.
- Hay, D. G., Sathasivam, K., Tobaben, S., Stahl, B., Marber, M., Mestril, R., Mahal, A., Smith, D. L., Woodman, B. & Bates, G. P. (2004) *Hum. Mol. Genet.* **13**, 1389–1405.
- Mitsui, K., Nakayama, H., Akagi, T., Nekooki, M., Ohtawa, K., Takio, K., Hashikawa, T. & Nukina, N. (2002) *J. Neurosci.* **22**, 9267–9277.
- Ishihara, K., Yamagishi, N., Saito, Y., Adachi, H., Kobayashi, Y., Sobue, G., Ohtsuka, K. & Hatayama, T. (2003) *J. Biol. Chem.* **278**, 25143–25150.
- Cowan, K. J., Diamond, M. I. & Welch, W. J. (2003) *Hum. Mol. Genet.* **12**, 1377–1391.
- Santoro, M. G. (2000) *Biochem. Pharmacol.* **59**, 55–63.
- Morimoto, R. I. (1998) *Genes Dev.* **12**, 3788–3796.
- Rimoldi, M., Servadio, A. & Zimmarino, V. (2001) *Brain Res. Bull.* **56**, 353–362.
- Batulan, Z., Shinder, G. A., Minotti, S., He, B. P., Doroudchi, M. M., Nalbantoglu, J., Strong, M. J. & Durham, H. D. (2003) *J. Neurosci.* **23**, 5789–5798.
- Kieran, D., Kalmar, B., Dick, J. R., Riddoch-Contreras, J., Burnstock, G. & Greensmith, L. (2004) *Nat. Med.* **10**, 402–405.
- Auluck, P. K., Chan, H. Y., Trojanowski, J. Q., Lee, V. M. & Bonini, N. M. (2002) *Science* **295**, 865–868.
- Kikuchi, S., Shinpo, K., Takeuchi, M., Tsuji, S., Yabe, I., Niino, M. & Tashiro, K. (2002) *J. Neurosci. Res.* **69**, 373–381.
- Waza, M., Adachi, H., Katsuno, M., Minamiyama, M., Sang, C., Tanaka, F., Inukai, A., Doyu, M. & Sobue, G. (2005) *Nat. Med.* **11**, 1088–1095.